

THE USE OF NEAR-INFRARED REMOTE SENSING IN THE DETECTION OF
CLANDESTINE HUMAN REMAINS

by

Marilyn E.R. Isaacks, B.A.

A thesis submitted to the Graduate Council of
Texas State University in partial fulfillment
of the requirements for the degree of
Master of Arts
with a Major in Anthropology
December 2015

Committee Members:

Daniel J. Wescott, Chair

M. Katherine Spradley

Michelle D. Hamilton

Ken Mix

COPYRIGHT

by

Marilyn E.R. Isaacks

2015

FAIR USE AND AUTHOR'S PERMISSION STATEMENT

Fair Use

This work is protected by the Copyright Laws of the United States (Public Law 94-553, section 107). Consistent with fair use as defined in the Copyright Laws, brief quotations from this material are allowed with proper acknowledgement. Use of this material for financial gain without the author's express written permission is not allowed.

Duplication Permission

As the copyright holder of this work I, Marilyn E.R. Isaacks, authorize duplication of this work, in whole or in part, for educational or scholarly purposes only.

DEDICATION

I would like to dedicate this paper to my mom and dad. Without their constant support and love, I don't think I could have made it through the first week of grad school. This is also dedicated to my best friend Randi, who very bluntly reminded me how much I love anthropology when I was too stubborn to acknowledge it myself. If not for you, my life might have been very different today.

ACKNOWLEDGEMENTS

I would like to thank my advisor, Dr. Daniel Wescott, for his guidance, patience, and good humor throughout this process. It was a comfort to know that his door was always open and that I would never be steered in the wrong direction, particularly during the most arduous days of data collection and analysis.

This research could not have been possible without grants, for which I thank Texas State for both the University Research Enhancement Program grant provided to Dr. Wescott and the Graduate Research Scholarship I was provided.

I would also like to express my gratitude to JP Fancher for his constant support and friendship, especially during data collection. I would like to acknowledge Dr. Jacqui A. Peterson, who graciously let me use her laboratory to process my samples and who took time out of her busy schedule to perform the chemical analysis used in my research. Finally, I would like to thank Gene Robinson and RP Flight Systems for performing the flyovers, creating the images of FARF, and being so accommodating throughout the past three years.

TABLE OF CONTENTS

	Page
LIST OF TABLES	viii
LIST OF FIGURES	ix
LIST OF ABBREVIATIONS	x
ABSTRACT	xi
 CHAPTER	
I. INTRODUCTION	1
Research Problem and Purpose	1
Research Questions	4
Background.....	5
Decomposition Processes and Chemical Alterations in the Soil.....	5
Spectral Analysis and the Search for Clandestine Human Remains	8
II. MATERIALS AND METHODS.....	12
Sample Size	12
Near-Infrared (NIR) Imaging	14
Materials	14
Confounding Variables.....	15
Hypothesis Testing	17
Supplementary Data	18
Soil Sampling	18
Ash-Free Dry Weight (AFWD) Analysis.....	19
Non-Purgeable Organic Carbon (NPOC) and Total Dissolved Nitrogen (TDN) Analysis	20
Statistical Tests	21
III. RESULTS	24
Do CDIs Have a Unique NIR Spectra and Soil Signature?.....	24
How Long After Death Can CDIs Be Seen Using NIR?.....	25

How Well Does Each Image Perform? Can People Successfully Find CDIs?	28
Do Animal Remains, Churned Soil, or Waterlogged Areas Present a Signature Similar to CDIs?.....	31
Animal Remains	31
Churned Soil	31
Waterlogged Areas	31
Does Seasonality Affect the Strength of the NIR Signature and the Amount of Organic Content in the Soil?	32
Is the Signature Correlated with Soil Organic Matter (SOM), NPOC, or TDN?	33
Univariate	33
Multivariate	37
IV. DISCUSSION AND CONCLUSIONS	38
Do CDIs Have a Unique NIR Spectra and Soil Signature?.....	38
How Long After Death Can CDIs Be Seen Using NIR?.....	39
How Well Does Each Image Perform? Can People Successfully Find CDIs?	42
Do Animal Remains, Churned Soil, or Waterlogged Areas Present a Signature Similar to CDIs?.....	47
Does Seasonality Affect the Strength of the NIR Signature and the Amount of Organic Content in the Soil?	48
Is the Signature Correlated with SOM, NPOC, or TDN?	49
Experimental Design	51
Conclusions	52
APPENDIX SECTION	56
WORKS CITED	81

LIST OF TABLES

Table	Page
2.1. Total sample size for each analysis	13
3.1. Descriptive statistics for true placements versus control sites by variable.....	25
3.2. Percentage of placements correctly identified by observers I, II, and III	28
3.3. Percentage of correctly identified placements for observers I, II, and III, separated by year of placement	30
3.4. Descriptive statistics for each season by variable	33

LIST OF FIGURES

Figure	Page
1.1. Aerial imagery of a section of the Forensic Anthropology Research Facility (FARF) at Texas State University using normal and NIR photography	3
1.2. Cadaver decomposition island with surrounding opportunistic flora.....	6
2.1. Specifications and dimensions of the Spectra Flying Wing.....	15
2.2. Flowchart of research objectives	23
3.1. Plotted variation in standardized greyscale value between controls and true placements	24
3.2. Standardized greyscale value versus days since placement	26
3.3. Standardized greyscale value versus days since placement	27
3.4. Standardized greyscale value versus percentage of SOM in the soil	34
3.5. Standardized greyscale value versus NPOC.....	35
3.6. Standardized greyscale value versus TDN	36
4.1. Examples illustrating the progression of CDI presentation types in the NIR spectrum	41
4.2. Examples illustrating CDI reflectance when cadaver is <i>in situ</i>	41
4.3. Images of FARF produced using automatic exposure and shutter priority	43

LIST OF ABBREVIATIONS

AFDW	Ash-Free Dry Weight
BMI	Body-Mass Index
C:N	Carbon-to-Nitrogen Ratio
CDI	Cadaver Decomposition Island
DDW	Double Distilled Water
DOC	Dissolved Organic Carbon
DON	Dissolved Organic Nitrogen
EO	Electro-Optical, or Visible
FAA	Federal Aviation Administration
FARF	Forensic Anthropology Research Facility at Texas State
NIR	Near Infrared
NPOC	Non-Purgeable Organic Carbon
ORPL	Osteology Research and Processing Laboratory
PMI	Postmortem Interval
SDV	Standardized Darkness Value
SOM	Soil Organic Matter
TDN	Total Dissolved Nitrogen
UAS	Unmanned Aircraft System

ABSTRACT

Most commonly, searches for clandestine remains have utilized time-consuming methods such as line searches that require the support of many individuals to scour a typically large area. While these methods do yield results, they take time to execute, and in certain places may actually prove dangerous for the participants. Many additional methods have been tested and utilized in the recovery of human remains, including the use of metal detectors, aerial photography, and ground-penetrating radar, which can be time consuming and expensive. Only in recent years has the use of near-infrared imagery been experimented with as a means of uncovering clandestine graves and surface remains. As human remains decompose, a large amount of organic matter enters into the surrounding soil, forming a cadaver decomposition island (CDI). Because soils that are organically rich have a different reflectance signature than nearby unaffected soils when viewed with near-infrared (NIR) imaging, it is likely that by using NIR photography and drone technology, clandestine remains may be recovered more quickly and more efficiently than has previously been possible. Because NIR photographs can be obtained using small, remotely controlled aircraft or aerial drones, large areas can be surveyed for clandestine remains remotely, thereby minimizing the need to involve a substantial group of people in the search. In so doing, potentially dangerous locations can be searched without great risk, disturbances to forensically significant sites will be minimized, and the area that personnel must search will be reduced and more precisely understood.

The present study explores the utility and longevity of near-infrared cameras mounted to Unmanned Aerial Systems (UAS) in the detection of clandestine human remains deposited on the surface. Aerial NIR photographs and soil samples were compiled from 104 identifiable CDIs (i.e., the fertile soil area below and surrounding a decomposing cadaver) at the Forensic Anthropology Research Facility at Texas State University in San Marcos, Texas. Results indicate that CDIs have a unique NIR spectra signature that can be successfully utilized to find clandestine remains.

I. INTRODUCTION

It is the last day of data collection in the field. I and another graduate student are spending the morning mapping as many placements (i.e., cadaver surface depositions) as possible so that we may begin to evaluate our individual data. Trudging through the wet grass on a cold and overcast day, we manage to find 89 of the 104 placements we had previously discovered during our first round of soil sampling several months prior. Returning alone to the field the following day, I discover 10 more placements – some of which neither of us had discovered even at the beginning of our research. Although each of us has spent an enormous amount of time in the field searching for placements, and although the placements are each marked with labeled wooden stakes, finding them all on a given day – or even finding the same set on two separate endeavors – is almost impossible from the ground. Because even clearly marked placements can be difficult to find in the field, it is clear that a new methodology for finding clandestine human remains in the field would be helpful in future search and recovery endeavors.

Research Problem and Purpose

Forensic anthropologists assist law enforcement during investigations by developing biological profiles from skeletal remains and aiding in search and recovery efforts. Most commonly, searches for clandestine remains have utilized time-consuming methods such as line searches that require the help of many individuals to scour a typically large area. While these methods do yield results, they take time to execute, and in certain places may actually prove dangerous for the participants (Kalacska and Bell

2006). Many additional methods have been tested and utilized in the search of human remains, including the use of metal detectors, aerial photography, and ground-penetrating radar (Ruffell et al. 2009). Yet only in recent years has the use of near-infrared imagery been experimented with as a means of uncovering clandestine graves (Kalacska and Bell 2006; Kalacska et al. 2009).

While “clandestine” remains typically refers to the hiding or secret placement, in this thesis the term is used more generally to refer to bodies on the ground surface or below ground surface for burial whose location is unknown to the searchers. This could be the result of the body being hidden to help conceal a crime or the unknown location of the body of an individual that died, such as a border crosser.

As human remains decompose, a large amount of organic matter enters into the surrounding soil, forming a cadaver decomposition island (Carter et al. 2007). According to Kalacska et al. (2009), soils that are organically rich have a different reflectance signature than nearby unaffected soils when viewed with near-infrared (NIR) imaging (Figure 1.1). Therefore, it is likely that clandestine remains may be recovered more quickly and efficiently than previously possible by using NIR photography and drone technology (Kalacska et al. 2009). Previous photos taken using NIR cameras at the Forensic Anthropology Research Facility (FARF) show evidence of body placement more clearly than do standard photos, highlighting anomalies indicating that a body was once present at a site even after it has been removed (Figure 1.1). Because NIR photographs can be obtained using aerial drones, large areas can be surveyed for clandestine graves remotely, thereby minimizing the need to involve a substantial group of people in the search. In so doing, potentially dangerous locations can be searched



Figure 1.1 Aerial imagery of a section of the Forensic Anthropology Research Facility (FARF) at Texas State University using normal (A) and NIR (B) photography. The NIR image more clearly shows the outline of the purge stains around the body (white circle), and the previous location of a surface decomposition site (dash circle).

without risk, disturbances to forensically significant sites will be minimized, and search areas will be reduced and more precisely understood.

The purpose of the present study is to help develop and test a novel method of using NIR remote sensing to aid search teams in locating and identifying clandestine human remains. Clandestine remains are here defined as cadavers – either buried or left on the surface – that are missing and require a search to discover. This thesis will explore the utility of remote sensing techniques using NIR photography as a tool for discovering clandestine surface deposits and human decomposition sites. Three primary goals will be addressed in this thesis. First, I will determine if CDIs can be detected and differentiated from natural features in Central Texas using NIR remote sensing techniques. Second, I

will examine if the strength of the CDI signal correlates with the organic chemistry of the CDI soil. Finally, I will investigate how long after death the CDI can be detected using NIR imaging as well as how they change over time.

Research Questions

The first null hypothesis for this study is that soils associated with decomposing human remains do not have an NIR spectra signature that can be differentiated from natural soils in Central Texas. This will be determined by evaluating the number of positive, negative, and false positive detections on the images. The alternative hypothesis is that soils with decomposing human remains do have a unique NIR spectra signature that is detectable using remote sensing. Here, the independent variable is the concentration of organic material in the soil determined by a soil test. The dependent variable is the NIR spectra signature of the soil measured using the greyscale value of the photograph obtained in Adobe Photoshop Elements 12®. If the null hypothesis is rejected, then the study will focus on the relationship between the NIR signature and soil nitrogen and carbon levels and determining how long the signature endures and if it changes with the postmortem interval (PMI). The working hypothesis is that there is a measurable timetable for this method that can be systematically predicted and tested based on chemical changes in the soil.

Background

Decomposition Processes and Chemical Alterations in the Soil

Human cadaver breakdown upon death is comprised of three major activities: autolysis, putrefaction, and decay (Benninger et al. 2008; Tibbett and Carter 2008). Autolysis, or cell destruction within the body, can begin moments after death. The anaerobic environment that this process facilitates in turn makes way for putrefaction, wherein acids and gases from the body are released causing the cadaver to darken, emit an odor, and begin to bloat (Statheropoulos et al. 2005; Tibbett and Carter 2008). Decay begins when “the integrity of the skin [is compromised, leading] to ruptures that allow oxygen back into the cadaver,” thereby facilitating the breakdown of the body (Tibbett and Carter 2008: 31). When a human body is left to decompose above ground, it undergoes this dynamic process while in contact with the ground, temporarily altering the matter directly beneath the body and immediately surrounding it. Further, because the cadaver is left to decompose outside, it is exposed to a greater amount of insect and scavenger activity (Bohun et al. 2010). The introduction of maggots to the body from fly larvae facilitates rapid breakdown of the remains as maggots consume and further degrade body tissues (Carter et al. 2007). The resulting area of affected soil is called a cadaver decomposition island. This process releases a huge amount of organic material into the soil as the body purges, the effects of which may linger for up to seven years after the placement of the body (Benninger et al. 2008). Initially, the area directly affected by the efflux of purge is characterized by the death of all underlying plant material and the darkening of the gravesoil in an approximate oval around the body. After a period of about 80 days postmortem, opportunistic plant life will make use of the

increased organic material in the soil and grow at amplified rates in the area surrounding the CDI (Carter et al. 2007). During the two years following the death and placement of the cadaver, the “richness and diversity” of floral species at the CDI continue to increase as a result of this influx of opportunistic flora (Towne 2000: 231) (Figure 1.2).



Figure 1.2 Cadaver decomposition island with surrounding opportunistic flora. These plants take advantage of the efflux of organic material and grow larger and more quickly than nearby plant life.

As the macroscopic changes described above are occurring, so too are changes in the composition of the soil at a microscopic and chemical level. A study of ungulate carcass decomposition performed by Towne (2000) indicated that inorganic nitrogen and phosphorous levels were significantly higher at the CDI than at equivalent control sites one year after placement, while pH levels were significantly lower at the CDI at this time. Similarly, a study performed by Aitkenhead-Peterson et al. (2012) on two adult human

cadavers (one exposed to scavenging, the other not) at 248 and 288 days postmortem, respectively, indicates a lower pH and higher levels of orthophosphate-P at the CDIs than at the control soils. That study also concluded that levels of dissolved organic carbon (DOC), dissolved organic nitrogen (DON), nitrate, calcium, and potassium were significantly higher at the CDI than at equivalent control sites (Aitkenhead-Peterson et al. 2012).

When bodies are left exposed to the elements, scavenger activity also has a role to play in the creation of a CDI. Several studies have shown that scavenger activity can noticeably alter the extent of the CDI around a body. Aitkenhead-Peterson et al. (2012: 133) demonstrated that allowing a body to be exposed to scavenging “will increase the spatial extent of the CDI for some chemical constituents, and furthermore, movement of body parts by scavengers will create hot spots of concentrated chemical constituents around the gravesite.” Towne (2000) also noted that during warmer seasons, the CDI of cadavers is often stronger and larger due to the restricted period during which scavengers may reach the cadaver before it has decomposed. The size of the cadaver prone to scavenging is also critical. Juvenile remains may create a small or negligible CDI, because scavengers can more easily drag off and disperse juvenile remains than adult remains because of their small size and low weight (Carter et al. 2007; Towne 2000). Adult remains, being larger and heavier, tend to be consumed largely *in situ*, with only smaller parts being dragged a significant distance from the placement site (Carter et al. 2007). In cases where scavenging contributes to the distribution of disarticulated remains, understanding how the CDI is altered and the potential spread of the remains away from the CDI becomes critically important to recovery efforts. Finding the CDI

provides a central point from which to begin the search and also allows for soil testing that may provide information about the postmortem interval.

Spectral Analysis and the Search for Clandestine Human Remains

The near-infrared spectrum spans the 700 to 1300 nanometer (nm) range of the electromagnetic spectrum and lies between the visible (400 – 700 nm) and shortwave infrared (1300 – 2500 nm) spectra (Kalacska and Bell 2006). In regard to plants, NIR reflectance is largely determined by the internal structure of the leaves (Kalacska and Bell 2006). Where soil is concerned, the reflectance signature is based primarily on the physical and chemical properties of the matrix, “mainly influenced by its constituents such as inorganic solids, organic matter, air and water” (Kalacska and Bell 2006: 4). The presence or absence of organic matter – the primary resource examined in the present study – affects the signature by differentially altering the reflectivity of the affected soil: “soils with high organic content, such as over 20%, will appear to be less reflective in the 400 – 2500 nm range, whereas soils with very little organic components will have an increased reflectance and prominent absorption features” (Kalacska and Bell 2006: 4). Further, NIR spectroscopy can be utilized to measure aspects of soil organic matter (Nagy and Konya 2009). For these reasons, it is critical to analyze the soil chemistry of CDIs to gain a deeper understanding of the interaction between the purge of organic material into the soil during cadaver decomposition and the corresponding reflectance signatures in the near-infrared spectrum.

Previous studies examining the utility of near-infrared spectroscopy are relatively few in number and have largely focused on agricultural applications rather than forensic. A study performed by Ben-Dor et al. (1997: 14) demonstrated the utility of visible, near-

infrared, and short wave infrared reflectance spectra for “monitoring the composting process in a real time mode” as well as for acquiring information about maturing organic matter. They further note that these spectra can be incredibly useful for examining even small changes during the composting process (Ben-Dor et al. 1997). A similar study conducted by McLellan et al. (1991: 1688) examined the utility of near-infrared spectroscopy in determining the “nitrogen, lignin, and cellulose concentrations of decaying foliage.” They conclude that the methodology works across all stages of plant decomposition and can provide more consistent measurements than traditional procedures (McLellan et al. 1991). The decomposition of leaf litter reintroduces essential nutrients into the soil, thereby sustaining growth; therefore the importance of accurately monitoring this process is of major value to agriculturalists (Bot et al. 2005). The benefits of near-infrared imaging, however, particularly when combined with remote sensing techniques span across both agricultural and forensic disciplines: in all cases, near-infrared remote sensing techniques provide a safe, less time-consuming, and inexpensive means of surveying often large areas of land (Kalacska and Bell 2006; Kalacska et al. 2009; McLellan et al. 1991; Xie et al. 2008). For forensic anthropologists and law enforcement officials, these benefits become particularly important during the search for clandestine human remains.

Explorations into the utility of hyperspectral imaging and remote sensing as a means of detecting clandestine human remains are few and date only to the last decade. The most prominent of these studies are those of Kalacska and Bell (2006) and Kalacska et al. (2009), wherein the authors utilized an experimental mass grave of cattle in Northwest Guanacaste, Costa Rica to test the efficiency and advantageousness of both

on-site and aerial spectral imaging. The spectral data collected from the aerial passes illustrate a clear advantage of near-infrared and shortwave infrared imaging over visible range imaging alone, as only the inclusion of the former two spectra allowed for a differentiation between control soils and the mass grave (Kalacska and Bell 2006; Kalacska et al. 2009). Further, the on-site spectral data collected from a handheld spectrometer allowed the researchers to differentiate between churned earth (as in a false grave) and true burials up to 16 months post-placement (when the study concluded) (Kalacska and Bell 2006; Kalacska et al. 2009).

A more recent study performed on pig (*Sus scrofa*) carcasses in Ottawa, Ontario examined the changes in visible through shortwave infrared spectra and to flora when chemicals associated with decomposition are introduced (Snirer 2013). Snirer (2013) concludes that within the first year of death and placement, the chemical composition of the soil matrix had only been significantly altered for surface placements, and not buried remains. Further, the author notes that “vegetation indices are a critical part” of searches for clandestine human remains – both for surface and burial placements – making visible and near-infrared hyperspectral imaging, which detect these vegetation changes, critical for forensic searches (Snirer 2013: 121).

Both of the above studies contribute a great deal of information to the limited bank of knowledge of spectral imaging and its utility in the field of forensic anthropology. The aim of the present research is to add to this knowledge by examining spectral data using cadavers and CDIs from a pre-existing longitudinal outdoor decomposition study that spans seven years (at the time of data collection), by incorporating unmanned drones to carry the NIR cameras, thereby reducing the cost and

manpower necessary to perform searches, and finally, by providing additional soil analysis of carbon and nitrogen levels and a large sample size ($n = 103$) of individually placed human cadavers. In combination with the existing studies, this research will expand research efforts by providing estimates of when NIR imaging ceases to be a useful methodology for forensic searches, by examining how well non-experts are able to pinpoint NIR hotspots, and by evaluating what organic and chemical signatures most affect the spectra signature.

II. MATERIALS AND METHODS

Sample Size

Aerial NIR photographs and soil samples were collected from 104 identifiable cadaver decomposition islands (i.e., the fertile soil area below and surrounding a decomposing cadaver) at the Forensic Anthropology Research Facility (FARF) at Texas State University in San Marcos, Texas (Appendix A). The soil is “slightly acidic (pH 6.3) and is classified as the Rumble series, a cherty clay loam with a surface layer comprised of 20% chert and limestone fragments and gravel” (Parks 2011: 19). All placements under examination in this study are donated human remains from the willed body donation program at Texas State’s Forensic Anthropology Center. Only surface depositions are considered in the present study. Because all burials at FARF are located in tree-covered areas and are therefore obscured from near-infrared photographs which reflect only surface material, buried remains were not examined in the present study. As knowledge of the date of placement for each cadaver is critical to the present analysis, placements without a readable identification number were excluded from the sample used for soil analysis. Some cadavers in the facility have been covered with tarps rather than wire cages, and these were also excluded from the soil analysis as the tarps obscure the CDI from the NIR cameras.

Two surface soil samples were taken from the center of each CDI on the day of the first drone flyover. Half of the soil samples collected from the center of each CDI were sent for analysis of organic materials at Texas A&M, Department of Soil and Crop Science, while the other half were burned in a muffle furnace at Texas State University to

estimate the amount of total organic carbon within each sample based on the difference between initial soil weight and the ash weight. Due to time constraints and limitations of available resources, 19 random samples were left out of the analysis performed by the laboratory at Texas A&M. Two samples were removed from the ash-free dry weight (AFDW) analysis, one due to growth of contaminating mold in the sample and one due to an insufficient amount of sample. No other samples were removed from the analyses.

Total n for each analysis is delineated in Table 2.1

Table 2.1. Total sample size for each analysis

Test	N
CDIs Sampled	103
Ash-Free Dry Weight Analysis	101
Chemical Analysis	84
Control Samples for Soil Analysis	12
Control Samples for NIR Strength Analysis	6

During the sample collection process, two soil samples were also taken from the edge of many of the CDIs, but regrowth of vegetation obscured the extent of the CDI in many of the older placements and so these samples were ultimately not utilized for the current analysis due to time and funding constraints. They have been placed in a freezer at the Osteology Research and Processing Laboratory (ORPL) at Texas State University for preservation should further analysis be desired in the future.

Near-Infrared (NIR) Imaging

Materials

Aerial NIR photographs of FARF were taken on July 25th and October 15th 2014. RP Flight Search Services photographed each area of FARF that contains or once contained human remains using cameras mounted on UAS. Areas of FARF not previously used were also photographed to determine whether natural disturbances create signatures similar to that of human decomposition. The aircraft utilized was a Spectra Flying Wing, an aircraft produced by RP Flight Systems that is optimized for carrying EO/IR optical and high-resolution digital imaging cameras (see Figure 2.1 for specifications of the aircraft). The aircraft was mounted with a Panasonic Lumix DMC-LX2 camera that had the bandpass filter replaced thereby allowing only the 660nm range of NIR to be recorded¹. The camera shoots in wide angle (28mm) and is triggered by the autopilot of the aircraft. The first set of images (July 25th, 2014) were shot using automatic exposure, while the second set of images (October 15th, 2014) were shot using shutter priority (i.e., the camera was programmed to use the fastest possible shutter speed to provide better detail on the ground) (Gene Robinson, personal communication).

¹ This is slightly below the true NIR range, but is considered as NIR for this study. The 660nm range, like true NIR, does capture variation in organic content, and is therefore appropriate for this study.


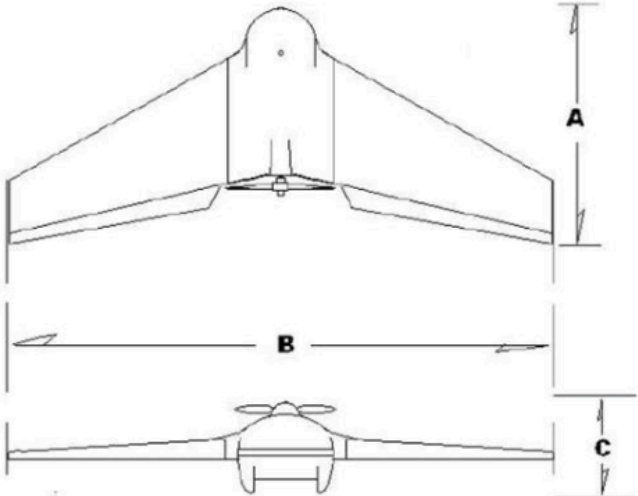
Spectra Flying Wing and Variants Optimum Configuration – 48" Wingspan Payload optional based upon mission criterion Copyright RPFlightSystems, Inc. © 2008			
Dimensions -- Scalability A – Depth: 16" to 32" B – Wingspan: 24" to 80" C – Height: 7" to 10"		Category Squad Level Force Multiplier	
		Specifications 48" Typical Wingspan <ul style="list-style-type: none"> • Construction: Composite ABS, Carbon Fiber, Fiberglass • Propulsion: Electric, three phase A/C. 90% efficiency, lithium polymer high density batteries • Empty Weight: 1.97 lbs • Payload: 2 – 4 lbs • All Up Weight: 4 lbs optimum up to 6 lbs max • Launch Type: Hand Launch • Retrieval/Landing: No special requirements • Climb Rate: 740 fpm • Cruise: 34 mph • Max: 55 mph • Stall: 14 mph (4 lb AUW) • Dwell Time: 45 minutes @ 50% cruise • Turnaround time: 3 min (all down/on station) • Typical Payload: Streaming EO/IR optical and high resolution digital imagery up to 10 megapixel 	

Figure 2.1. Specifications and dimensions of the Spectra Flying Wing (Obtained from the RP Flight Systems website [http://www.rpflightsystems.com/SpectraAP.html] and used with permission by Gene Robinson).

Confounding Variables

There are several confounding variables that could affect NIR spectra signatures and mimic the signature of a clandestine grave. Churned (as in a burial) or virgin soil, moisture, and nonhuman decomposition sites may all affect vegetation and light reflectance similarly to human decomposition sites. Thus, these disturbances may have an effect on NIR spectra signatures, potentially giving a reading other than dry or undisturbed soil. Cadaver body weight could also affect the NIR signature of CDIs, given that larger individuals tend to produce a broader, more concentrated soil stain than that of more slight individuals (Towne 2000). Finally, seasonality could affect CDI size

and depth, and therefore NIR strength, due to temperature fluctuations and the affect that this can have on decomposition rates and insect activity (Reed 1958; Rodriguez and Bass 1983; Vass et al. 1992).

Because there are several potential confounding variables that could present with NIR spectra signatures similar to that of cadaver decomposition islands (CDIs), it is important to include these variables in the study so that their effects may be noted. Therefore, approximately 30 minutes before each NIR photograph was taken, certain otherwise non-affected soil areas were saturated with approximately five gallons of water in a shape resembling that of a CDI. Four false graves (i.e., areas of disturbed soil without a body placement) had also previously been created, and several animal carcasses had been placed at FARF as part of previous studies. As a result, it was possible to examine these areas alongside the CDIs in each NIR photograph to test their similarity and to understand whether one can be distinguished from another. The effects of seasonality and body mass were examined statistically. Season of death was determined using date of placement for each donor. To examine the effect of body weight, stature and body weight were obtained from the donor files and converted to a body mass index (BMI). Body mass was used rather than weight, as the former provides more information about body fat or (in some rare cases) muscle mass than does the latter. To reduce observer bias, three individuals – including someone who is unfamiliar cadaver placements at FARF – examined each photograph to suggest anomalies indicative of CDIs. These extra measures minimized the effects (if any) that the confounding variables might have on determining the location of CDIs from NIR photographs.

Hypothesis Testing

To test the hypothesis that a measurable timetable for when the NIR method can be systematically predicted, the visual results of the NIR photographs must be converted into meaningful quantitative data. As the photos were taken at different times of the day, and in differing weather conditions (i.e., cloudy versus sunny), it was necessary to calibrate the values for each photo. This was achieved through the use of photographic white paper placed at FARF at each flyover, which equalizes the lighting of each photo so that they are not differentially altered by the circumstantial effects of the weather. Once the photos were obtained, Adobe Photoshop Elements 12® was used to convert each photo into gray scale, allowing the affected areas to be sampled using the eyedropper tool (Ajay Bedi 2013). The eyedropper tool provides a numeric value between zero (pure white) and 100 (black) that estimates the darkness of the sampled areas. For each CDI, five values (four from the perimeter and one from the center) were obtained using the eyedropper tool (zoom levels between 66.67% and 100%) and the average was taken. This diminished the opportunity for sampling error by ensuring that each darkness value was the result of the complete CDI, rather than of one small part of it. Each of the two photo sets were standardized prior to analysis using photographic white paper, which established a pure white (or “0”) baseline in the images. Using these values, independent t-tests can then be performed to estimate whether the NIR spectra signature of CDIs is significantly different from that of unaffected soil and whether this signature will fade predictably over time.

To test whether one exposure methodology (i.e., automatic shutter or shutter priority) performs more efficiently than the other, the success rates for each tester were

compared visually². These rates were derived from the total number of potential CDIs and the total number of selections made by the tester designated as “true positives.” These success rates were also subdivided by year to examine more fully how long after placement individuals may use NIR imaging to detect CDIs.

Supplementary Data

To supplement the UAS data, individual photographs of the soil and vegetation within a one-meter area of each placement were taken using a hand-held digital camera shooting in the visible light spectrum corresponding to the date of the first NIR aerial imaging. Had an uncertainty arisen as to the visual appearance of a CDI later in the study, these photos would have served as a record of the status of each CDI on the date of the first flyover. Data on how long each cadaver remained at FARF, when the cadavers were removed, and the BMI of each cadaver was also gathered. Using this data in conjunction with the aerial photos, estimates of how long the NIR signature of CDIs will last before they begin to resemble the surrounding unaffected soil was obtained.

Soil Sampling

Samples were taken using a LaMotte 1055 Model EP Soil Sampling Tube with a 1” core diameter. Each core contained five to eight centimeters of soil, approximating the seven-centimeter sampling methodology of Aitkenhead-Peterson et al. (2012). Where only the CDI remained, samples were taken from the middle of the CDI. In cases where bodies were still *in situ*, samples were taken from either the groin or the left armpit as these areas contain the highest concentrations of purge fluid and thus the greatest amount

² Given larger sample sizes, paired t-tests could be performed in the future during a more prolonged study.

of organic material (Aitkenhead-Peterson et al. 2012). Once taken, samples were placed in labeled medium flexible sample containers, hung on a wire in an outdoor covered shed, and allowed to air dry for two weeks before analyses were performed. Throughout the sampling and the analyses, special care was taken not to touch the samples themselves with bare hands to avoid contamination of the soil.

Ash-Free Dry Weight (AFDW) Analysis

Each sample was first prepared by grinding the soil using a mortar and pestle to break up large clusters of dirt, though not enough to completely pulverize the soil to powder. The samples were then transferred to canisters and placed in a dryer for at least 24 hours at 200°F to complete drying of the sample. Once drying was complete, each sample was weighed and transferred to a crucible and placed into a kiln for 24 hours at 800°F to burn off all organic carbon. After burning for at least 24 hours, the kiln was subsequently turned off and the samples were allowed to cool for 24 hours before being removed from the kiln and reweighed. Three measurements of weight in grams (g) were taken to perform this analysis: 1) the mass of the crucible, 2) the mass of the crucible and the soil before entering the kiln, and 3) the mass of the crucible and the soil once removed from the kiln. This allowed for the determination of the mass of the dry soil (M_D) using the equation,

$$M_D = M_{PDS} - M_P,$$

where M_{PDS} is the mass of the crucible and soil, and M_P is the mass of the crucible. After burning the mass of the burned soil ash (M_A) was calculated as

$$M_A = M_{PA} - M_P,$$

where M_{PA} is the mass of the crucible and the ashed soil. The mass of the organic matter

in the soil was then calculated using the equation

$$M_O = M_D - M_A$$

Finally, the organic content of the soil (OM) was calculated as

$$OM = \frac{M_O}{M_D} \times 100$$

To avoid cross-contamination of the soils, the materials used to process the soils – mortar and pestle, canisters, and crucibles – were washed with water and dish detergent and dried thoroughly before reuse. Because only nine samples could fit into the kiln at a time, the remaining samples were placed into a refrigerator until needed to halt any change in the soil chemistry that could confound the analysis.

Non-Purgeable Organic Carbon (NPOC) and Total Dissolved Nitrogen (TDN) Analysis

Before the chemical analysis of the soils could be performed, each sample had to be prepared by removing non-soil contaminants and homogenizing the texture of each sample. The samples were first ground using a mortar and pestle to break up large clusters of dirt, though not enough to completely powder the soil. The soil was then sieved to remove any remaining non-soil debris and larger soil clusters, and each sample was placed inside a paper bag that was labeled and stored until further preparation and analysis could be performed. Once this preliminary preparation was completed, approximately three grams of each sample was then measured and placed into a plastic test tube along with roughly 10 times that amount of double distilled water (DDW) (~30g). The soil and water mixture was then placed on a shaker to agitate the sample for 20-22 hours, homogenizing the mixture. Next, the samples were removed from the shaker in groups of eight and placed in a centrifuge to re-separate the heavier soil from the lighter water. This allowed the water from the sample to then be extracted and placed

into a new beaker. A dilute of DDW was then added to the extracted sample at approximately a one-to-one ratio. Once the samples were prepared, the analysis proceeded as follows:

Dissolved organic carbon (DOC) and total dissolved nitrogen (TDN) were measured using high-temperature Pt-catalyzed combustion with a Shimadzu TOC-VCSH and Shimadzu total measuring unit TNM-1 (Shimadzu Corp. Houston, TX, USA). Dissolved organic carbon were measured as non-purgeable carbon using USEPA method 415.1 which entails acidifying the sample and sparging for 4 min with C-free air (Aitkenhead-Peterson, personal communication).

Statistical Tests

Prior to any statistical testing, research objectives were clearly delineated (Figure 2.2). Statistical tests that would most efficiently and accurately answer each question were then chosen for each objective. To analyze whether CDIs have a unique NIR spectra signature, an unpaired t-test was calculated using the standardized greyscale values of the true placements and that of the control samples. Unpaired t-tests examine whether there is a significant difference between the means of the two groups in question, thereby examining whether the range of spectral signature values is significantly different between controls and true placements. Only samples that could be found in the images and accurately sampled using the eyedropper tool were taken into consideration for this analysis. Although the resulting sample size for the control sites is small ($n = 12$) in comparison to that of the true placements ($n = 82$), sample size for both groups is

sufficient to use a t-test. Similarly, to examine whether CDIs produce a unique chemical signature in the soil, unpaired t-tests were calculated using the organic content, NPOC, TDN, and C:N ratio values for the true placements versus the control samples. For each of these, sample sizes are sufficiently large (see above), making t-tests an appropriate measure.

Scatterplots were created and regression equations were created for each variable (organic content, NPOC, and TDN) against the standardized greyscale value to examine how well each variable individually explained the strength or weakness of the NIR spectra signatures of the CDIs. Similarly, a scatter plot was created using days since placement of each cadaver against the standardized greyscale value to estimate how much of the variation in standardized greyscale value can be explained by time. These individual plots are appropriate measures as they help to illustrate how well a single trait may explain NIR spectra signature strength. Multiple linear regressions were also run on all available variables to examine which variables have the greatest effect on NIR spectra signature strength and whether multiple variables together might improve the correlation. A stepwise function was used to eliminate variables that do not significantly improve the correlation or predict NIR spectra signature strength.

A MANOVA was run to examine the effect of seasonality on the strength of the NIR signature and the amount of organic content in the soil. Because there are multiple dependent variables [Organic Content, NPOC, TDN, and Standardized Darkness Value (SDV)] and a single independent variable with two groups (Season), a MANOVA is the most appropriate statistical test.

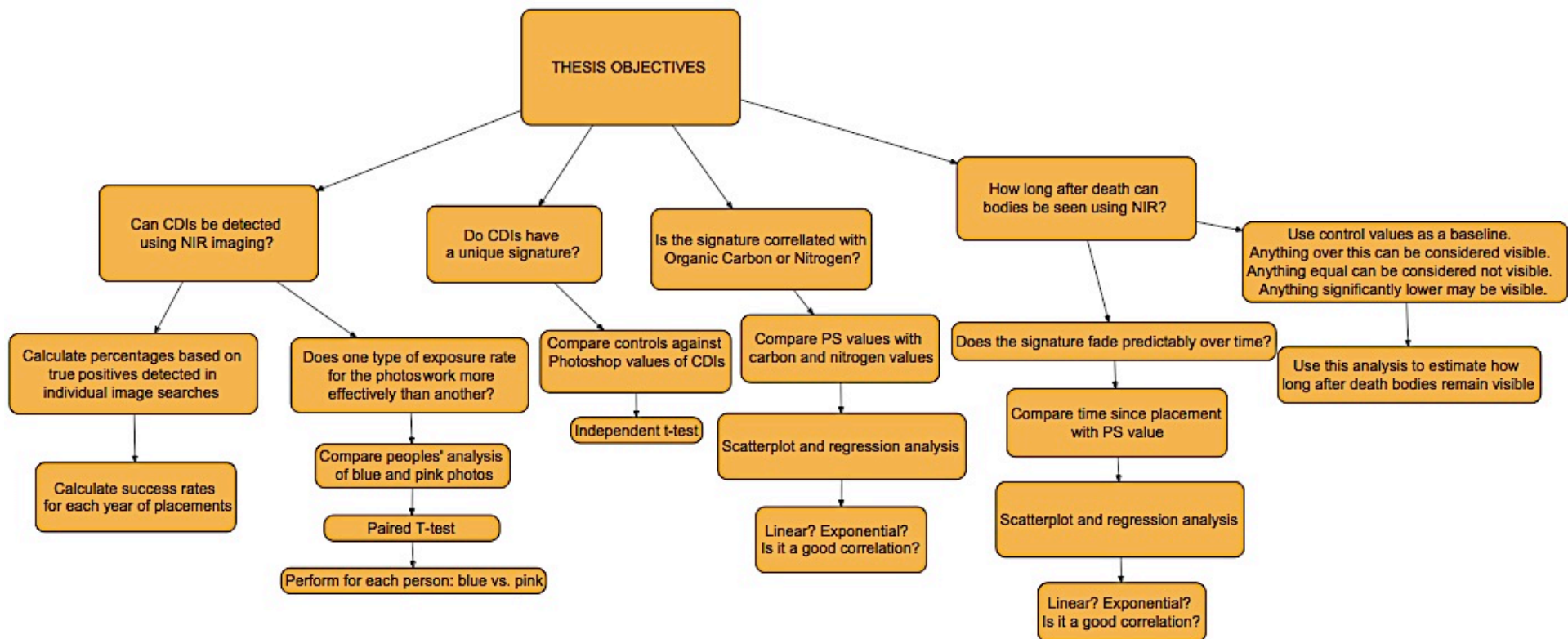


Figure 2.2. Flowchart of research objectives.

III. RESULTS

Do CDIs Have a Unique NIR Spectra and Soil Signature?

The standardized greyscale values (i.e., NIR spectra signature) of the true CDIs and the control samples are plotted in Figure 3.1. An unpaired t-test was used to examine the difference between the standardized greyscale values (i.e., NIR spectra signature) of the true placements and that of the control samples. Because the variances of the two groups are unequal (25.89 for CDIs and 0.70 for controls), a t-test assuming unequal variances was used. The results are significant at the $p < 0.01$ level.

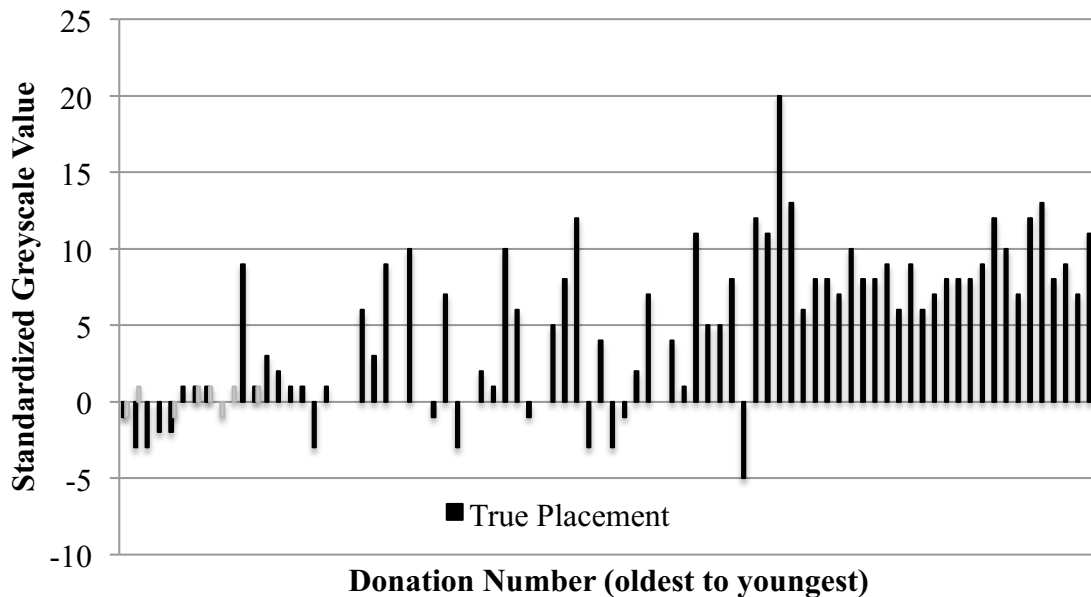


Figure 3.1. Plotted variation in standardized greyscale value between controls and true placements.

To examine whether there is a reasonable difference in the soil chemistry of the true placements versus the control sites, descriptive statistics were calculated for both groups, separated by variable (Table 3.1). Means were then compared using unpaired t-tests. All tests are significant at the $p < 0.01$ level.

Table 3.1. Descriptive statistics for true placements versus control sites by variable¹.

Variable Type		Mean	Standard Deviation	N²
Organic Content	True Placement	11.79	4.89	68
	Control	8.74	2.14	12
	Total³	11.33	4.71	80
Non-Purgeable Organic Carbon	True Placement	2385.07	2498.01	68
	Control	279.79	54.65	12
	Total	2069.27	2421.75	80
Total Dissolved Nitrogen	True Placement	320.82	303.90	68
	Control	33.10	5.41	12
	Total	277.67	298.36	80
Carbon-Nitrogen Ratio	True Placement	9.51	8.32	68
	Control	8.46	1.02	12
	Total	9.35	7.68	80
Standardized Darkness Value	True Placement	4.74	5.08	68
	Control	0.17	0.83	12
	Total	4.05	4.97	80

¹True Placement and Controls are statistically different ($P < 0.01$) for all variables.

²Sample sizes are lower than expected for some variables because SPSS removes rows with empty cells from the analysis.

³“Total” rows represent the grouped means, standard deviations, and sample sizes for each variable.

How Long After Death Can CDIs Be Seen Using NIR?

Using the greyscale values obtained in Photoshop®, the control samples were taken as a baseline. This baseline indicates the range of which any given section of unaffected soil should differ from other nearby unaffected soil. Values significantly above or below this baseline should be visible in the NIR spectra photographs to the naked eye. The values taken at the center of the placement (or section of control soil) were subtracted from an averaged value taken from the unaffected soil in the immediate

vicinity to obtain a standard measurement of NIR visibility.

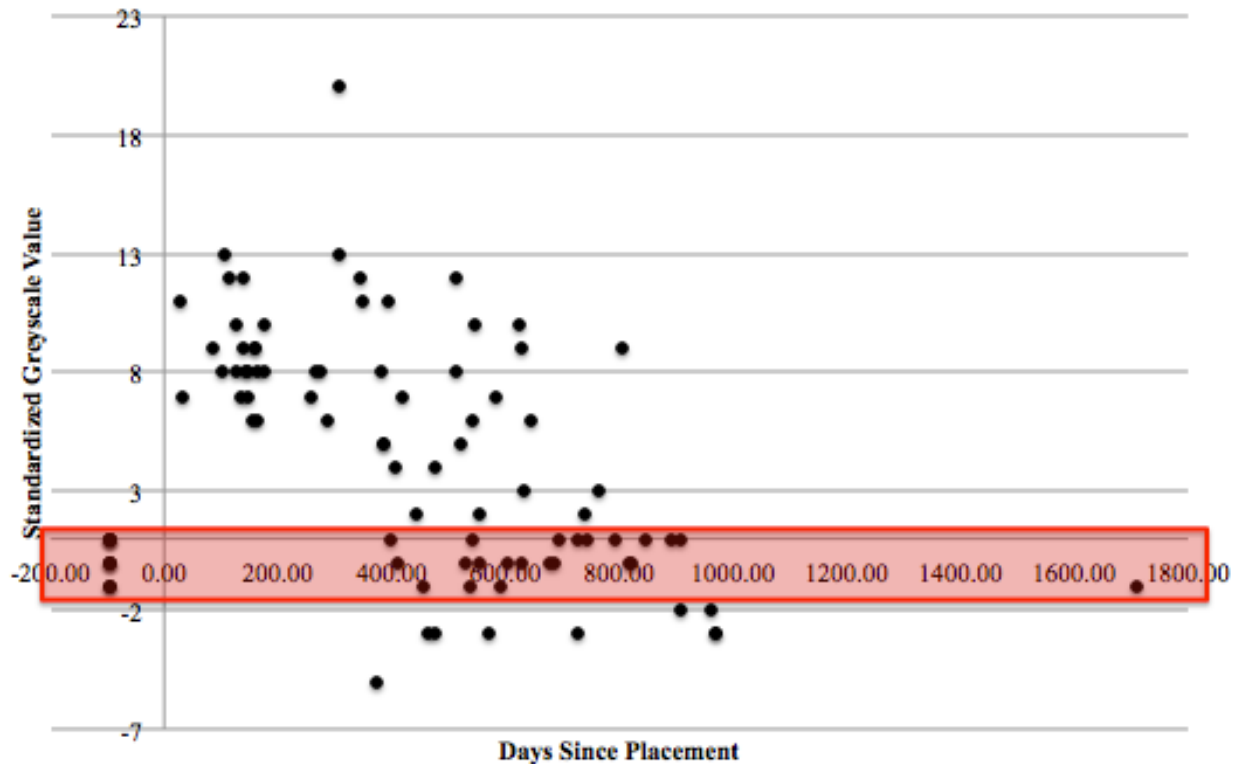


Figure 3.2. Standardized greyscale value versus days since placement. Bar indicates the baseline values at which CDIs are not distinguishable from the surrounding soil. Control samples are to the left of the y-axis line.

Figure 3.2 illustrates the distribution of standardized greyscale values against days since the body was placed on the surface ($n = 81^3$). CDIs that are younger than approximately 650 days old – but that are at least a week old – show consistently higher values than the baseline (-1 to 1), with few exceptions. CDIs that have been in place for more than 700 days show a distinct drop in greyscale value, clustering more closely around the baseline. Between about 400 to 1000 days since placement, it must also be noted that many CDIs present with negative values far below the baseline. This

³ Although 110 total placements were found in the field, only 82 could be accurately sampled for darkness value in the first NIR image as tree cover obscured certain placements in the visible light image making them impossible to map.

illustrates some overlap between the maximum efficiency time period and the period in which negative values may begin to appear.

To test whether the signature fades predictably over time, a scatterplot was created comparing the standardized greyscale values against the number of days since the body was initially placed. The R^2 was calculated based on the linear regression generated for this data, illustrated in Figure 3.3. The results indicate that 38% of the variation in NIR signature can be explained by time.

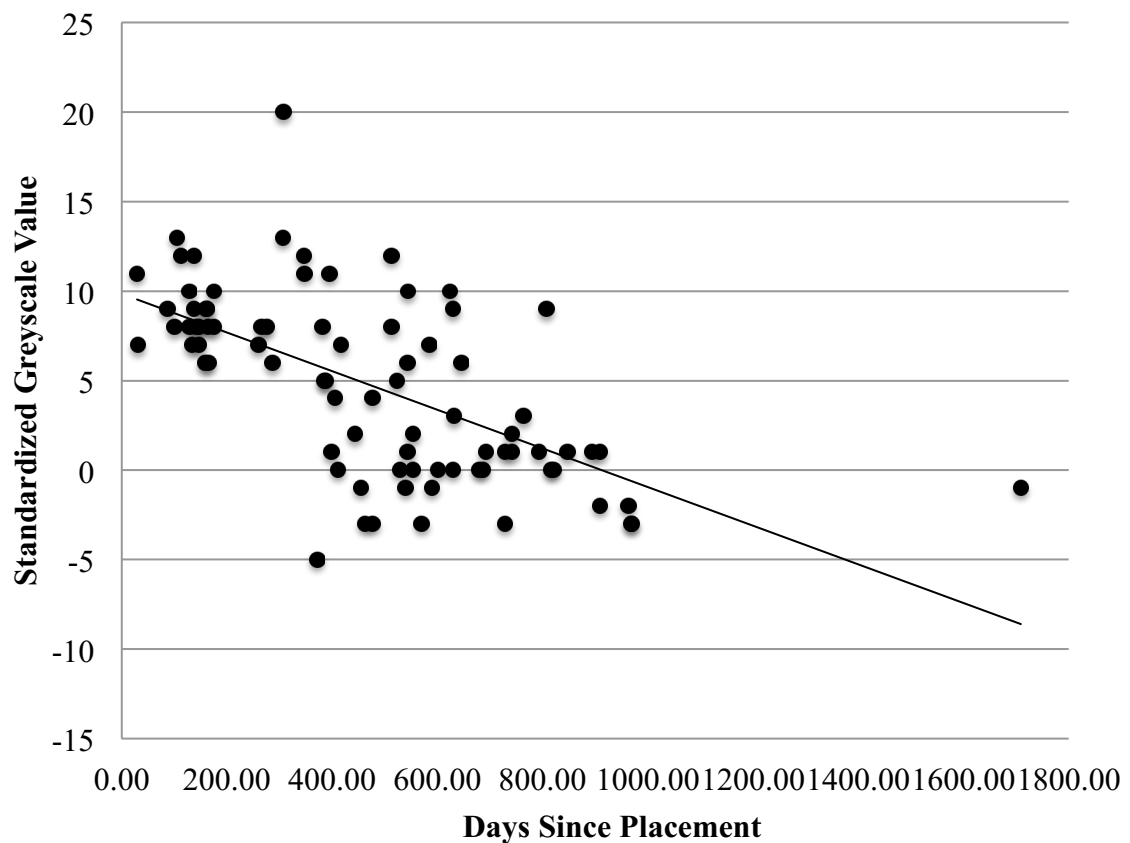


Figure 3.3. Standardized greyscale value versus days since placement. Linear regression ($y = -0.0108x + 9.8415$) was applied to the data and an R-squared value produced ($R^2 = 0.3853$).

How Well Does Each Image Perform? Can People Successfully Find CDIs?

To examine whether individuals could successfully discover CDIs using the NIR images produced from drone flyovers, three people with differing levels of knowledge of the facility were asked to circle anomalies in both images that they considered to be potential CDIs. Using the total number of placements available for each image⁴ [n(Automatic Exposure) = 87, n(Shutter Priority) = 89) percentages were then calculated based on how many true placements the individuals found. The results are shown in Table 3.2.

Table 3.2. Percentage of placements correctly identified by observers I, II and III.

	Observer		
Shutter Method	I	II	III
Automatic Exposure	51.7	28.7	56.3
Shutter Priority	34.8	14.6	30.3

Because the sample size is so small, no statistical comparison could be performed with accuracy to determine which image, and therefore which exposure method performs best. Visually, however, the data may be compared for differences in performance for each image. It may be noted that for each individual, the first set of images (automatic exposure) resulted in a higher percentage of correct identifications.

⁴ Although 110 total placements were found, tarped cages and bodies placed under trees were excluded, as they could not be accurately placed on a map of the facility or be viewed by the drone. For this analysis alone, the Operation Identification cage was included as part of the total sample, as this cage does represent a site of human decomposition. These adjustments account for the discrepancies in sample size for this analysis.

In order to examine whether placements become more difficult to identify in the NIR spectra over time, observer success rates were calculated for each year, from 2009 to 2014 (Table 3.3). Although the facility has been operational since 2008, no placements were discernible in the field during this year. Similarly, because no placements from 2010 were found, this year was also excluded from the analysis. Visual comparisons on the yearly success rates were used to estimate if a given exposure method performs better than another as the placements age.

Table 3.3. Percentage of correctly identified placements for observers I, II, and III¹, separated by year of placement

<u>2009 Automatic Exposure</u>			
Observer	Found	Total	Percent Correct
I	0	1	0%
II	0	1	0%
III	0	1	0%
<u>2011 Automatic Exposure</u>			
Observer	Found	Total	Percent Correct
I	0	3	0%
II	1	3	33%
III	0	3	0%
<u>2012 Automatic Exposure</u>			
Observer	Found	Total	Percent Correct
I	5	26	19%
II	5	26	19%
III	6	26	23%
<u>2013 Automatic Exposure</u>			
Observer	Found	Total	Percent Correct
I	17	35	49%
II	17	35	49%
III	21	35	60%
<u>2014 Automatic Exposure</u>			
Observer	Found	Total	Percent Correct
I	21	21	100%
II	2	21	10%
III	21	21	100%
		Overall Total: 86	

<u>2009 Shutter Priority</u>			
Observer	Found	Total	Percent Correct
I	0	1	0%
II	0	1	0%
III	0	1	0%
<u>2011 Shutter Priority</u>			
Observer	Found	Total	Percent Correct
I	0	3	0%
II	0	3	0%
III	0	3	0%
<u>2012 Shutter Priority</u>			
Observer	Found	Total	Percent Correct
I	4	27	15%
II	1	27	4%
III	5	27	19%
<u>2013 Shutter Priority</u>			
Observer	Found	Total	Percent Correct
I	10	38	26%
II	9	38	24%
III	5	38	13%
<u>2014 Shutter Priority</u>			
Observer	Found	Total	Percent Correct
I	16	19	84%
II	3	19	16%
III	16	19	84%
		Overall Total: 88	

¹Totals based on all placements found in the field, excepting tarped cages, those under trees, and the Operation Identification cage (since this has no specific year).

**Do Animal Remains, Churned Soil, or Waterlogged Areas Present a Signature
Similar to CDIs?**

Animal Remains

Four animal carcasses placed at FARF several months before the flyovers (exact dates unknown) were included in the area mapped and photographed by the UAS on each flight. Although one of the observers testing the images for anomalies did not note any of the animal carcasses significant for either image, the two remaining observers both took note of these anomalies in both images. These observers logged between 2 and 4 of these carcasses as significant for each flyover.

Churned Soil

Four false graves of churned soil, created long before each flyover (July 2013), were also included in the UAS mapped area that has been photographed in the NIR spectrum. Two of the three observers testing the images for anomalies noted these four false graves as potential areas of significance in both images. The third observer – who also did not pinpoint animal remains as significant – did not take note of the churned soil areas in either image.

Waterlogged Areas

To assess the potential problem of soil moisture, approximately 30 minutes before each NIR photograph was taken certain otherwise non-affected soil areas were saturated with approximately 5 gallons of water in a shape resembling that of a CDI. This area was noted using GPS coordinates and included in the mapped area photographed by the UAS. Despite warm and dry climatic conditions during the days of each flyover (average

temperature of about 85°F in July and 74°F in October), none of the testers discovered the false water grave or noted it as a potential anomaly.

Does Seasonality Affect the Strength of the NIR Signature and the Amount of Organic Content in the Soil?

A MANOVA was run using Organic Content, NPOC, TDN, and SDV as dependent variables and Season (divided into two groups: Spring/Summer and Fall/Winter) as the independent variable. Bartlett's Test of Sphericity demonstrates a sufficient correlation among the dependent variables ($X^2 = 1925.438$, $df = 9$, $p < 0.001$). There is not a statistically significant multivariate effect (Pillai's Trace = 0.173, $p = 0.085$), indicating that there is no difference between the groups of the independent variable on the variate. To further examine the effect of seasonality on decompositional soil chemistry, descriptive statistics generated from the MANOVA were examined visually, with no notable differences (Table 3.4).

Table 3.4. Descriptive statistics for each season by variable.

Season		Mean	Standard Deviation	N¹
Organic Content		8.74	2.14	12
	Fall/Winter	11.95	4.70	36
	Spring/Summer	11.61	5.17	32
	Total²	11.33	4.71	80
Non-Purgeable Organic Carbon		279.79	54.65	12
	Fall/Winter	2481.59	2624.92	36
	Spring/Summer	2276.48	2384.19	32
	Total²	2069.27	2421.75	80
Total Dissolved Nitrogen		33.10	5.41	12
	Fall/Winter	304.17	264.03	36
	Spring/Summer	339.56	346.72	32
	Total²	277.67	298.36	80
Standardized Darkness Value		0.17	0.83	12
	Fall/Winter	5.06	5.19	36
	Spring/Summer	4.38	5.01	32
	Total²	4.05	4.97	80

¹ Sample sizes are lower than expected because SPSS removes rows with empty cells from the analysis.

²“Total” rows represent the grouped means, standard deviations, and sample sizes for each variable.

Is the Signature Correlated with Soil Organic Matter (SOM), NPOC or TDN?

Univariate

To test whether the NIR reflectance signature is correlated with organic carbon or nitrogen, scatterplots were created comparing the standardized greyscale value against percentage of organic carbon, NPOC, and TDN. Figures 3.4 through 3.6 illustrate the results of these tests, demonstrating a poor correlation between NIR signature and percentage of SOM, but a stronger correlation between NIR signature and NPOC and TDN.

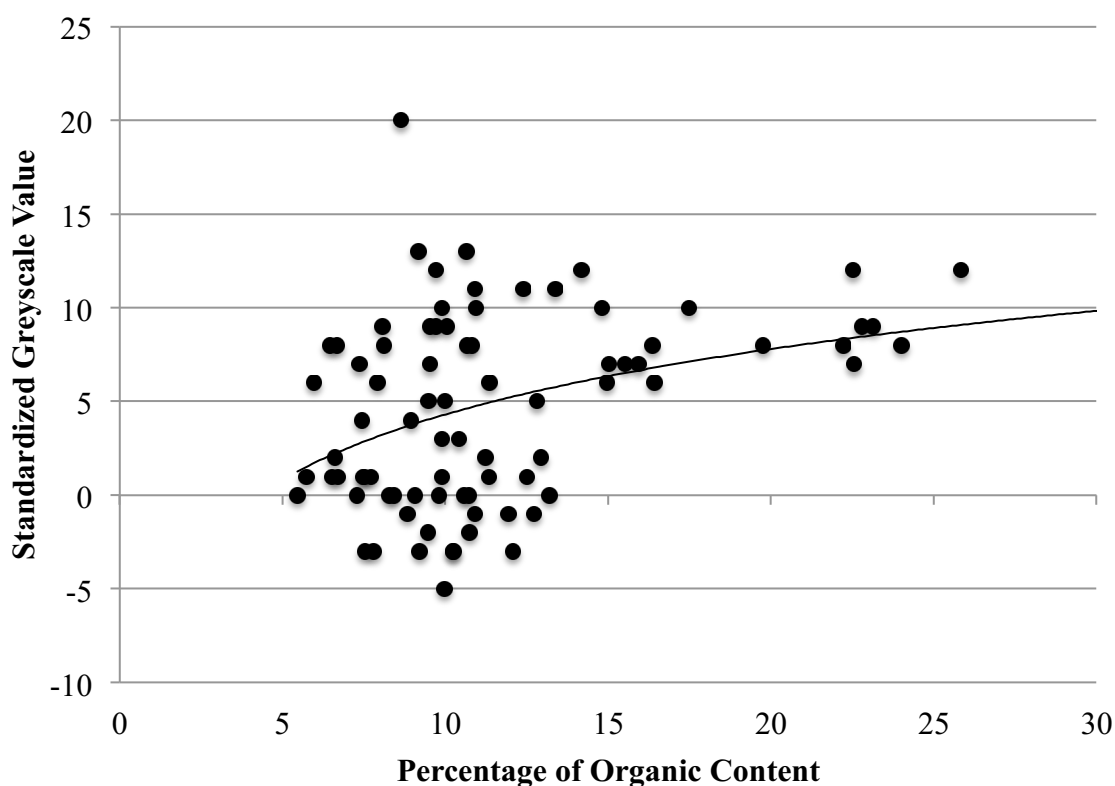


Figure 3.4. Standardized greyscale value versus percentage of SOM in the soil. Logistic regression ($y = 5.034\ln(x) - 7.2847$) was applied to the data and an r-squared value (0.1245) produced. Black dots represent the difference between the center and surrounding soil. The solid line is the log regression line.

The analysis of SOM (Figure 3.4) produces an r^2 value of 0.13 when a logarithmic equation is applied to the data.

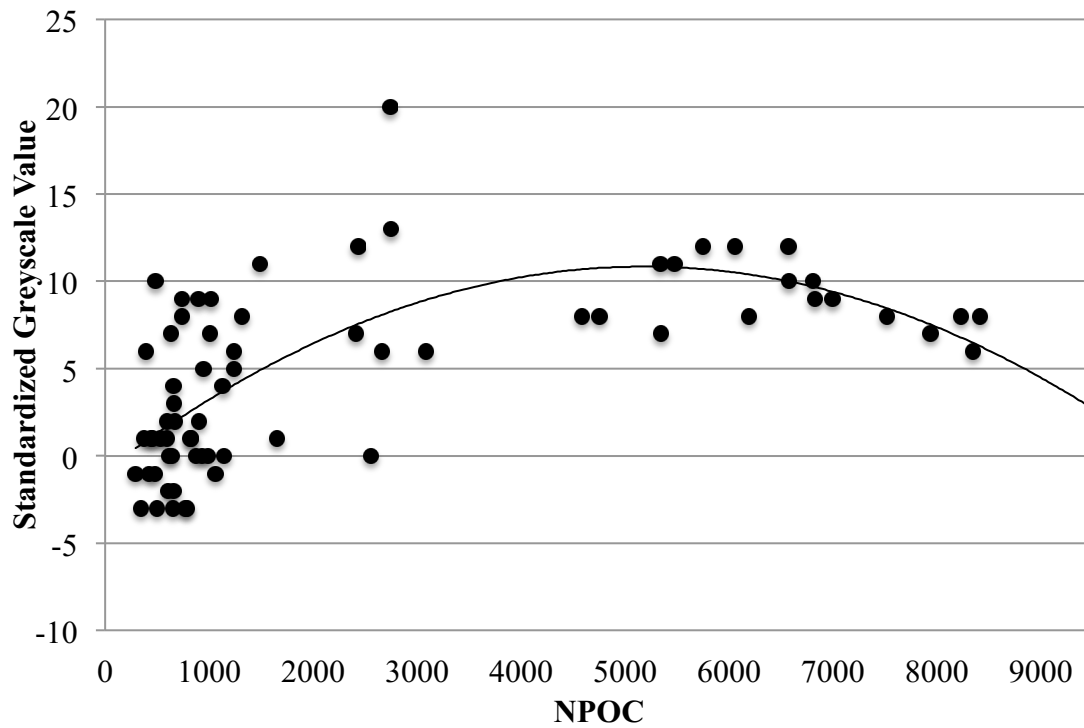


Figure 3.5. Standardized greyscale value versus NPOC. Polynomial regression ($y = -4\text{E-}07x^2 + 0.0045x - 0.8546$) was applied to the data and an r-squared value (0.47713) produced. Black dots represent the difference between the center and surrounding soil. The solid line is the polynomial regression line.

The analysis of NPOC (Figure 3.5) indicates an r^2 value of 0.48 using a polynomial equation.

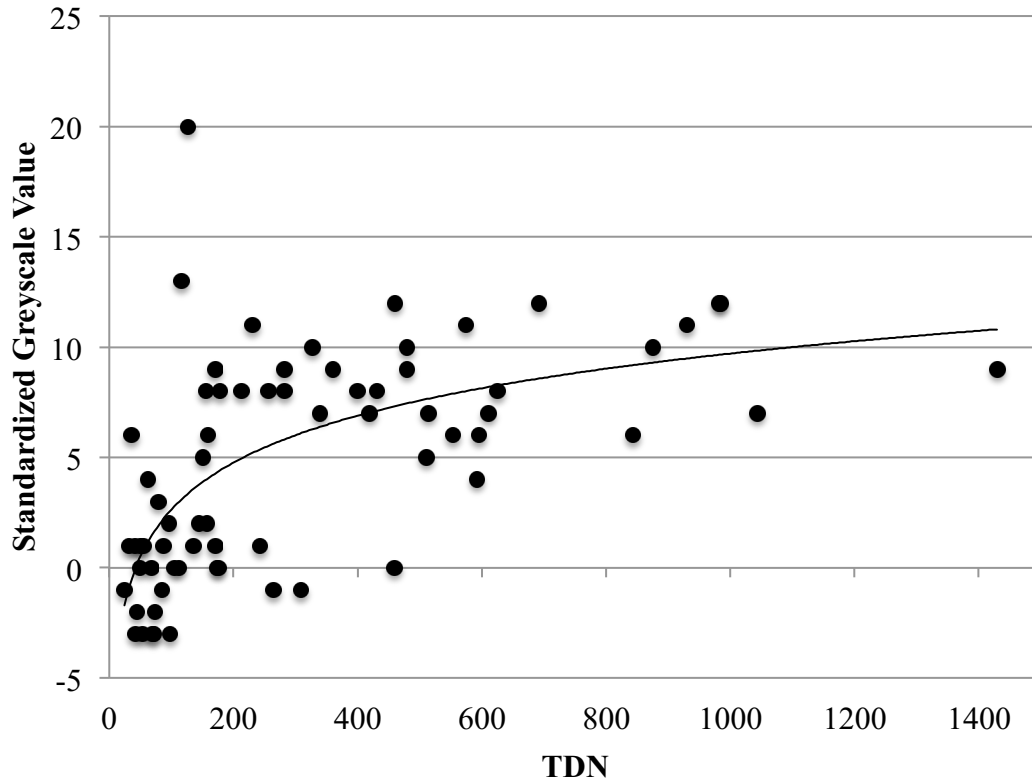


Figure 3.6. Standardized greyscale value versus TDN. Logistic regression ($y = 3.0735\ln(x) - 11.518$) was applied to the data and an r-squared value (0.38491) was produced. Black dots represent the difference between the center and surrounding soil. The solid line is the log regression line.

The analysis of TDN (Figure 3.6) indicates an r^2 value of 0.38 when fitted with a logarithmic trendline. When tested against other regression equations, polynomial regression best explained the correlation between standardized greyscale values and NPOC, while logarithmic regression best explained the correlation between standardized greyscale values and both SOM and TDN.

T-tests were run for each of the variables, separating between obese (BMI of 30 or greater) and not obese (BMI less than 30) individuals. None of these tests were significant ($p > 0.05$ for all variables). Regressions were also created to test the

correlation between BMI or weight (kg) and each of the above variables. No correlation was discovered between any variable and either BMI or weight.

Multivariate

When a stepwise multiple linear regression is run using SOM, organic carbon, total nitrogen, and body mass index (BMI) against the SDV, the correlation improves. The model that best predicts darkness value utilizes only SOM, organic carbon, and total nitrogen, eliminating BMI from the analysis. This regression equation explains 43.1% of the variation in SDV. An ANOVA analysis indicates that the model does significantly predict the dependent variable [$F(3, 58) = 14.647, p < 0.001$]. As indicated by the univariate analysis, the semipartial correlation confirms that NPOC individually accounts for the greatest explained variance in the dependent variable.

When the multiple linear regression is rerun with the variables above (including BMI) and days since placement, the resulting equation is dramatically different than the above. In this instance, running a stepwise function, the model that best predicts darkness value utilizes only TDN and Days Since Placement, eliminating all other variables from the analysis. The resulting regression equation explains 48.9% of the variation in SDV. An ANOVA analysis indicates that the model does significantly predict the dependent variable [$F(2, 59) = 28.222, p < 0.001$]. In this model, the semipartial correlation indicates that Days Since Placement individually accounts for the greatest explained variance in the dependent variable.

IV. DISCUSSION AND CONCLUSIONS

Do CDIs have a Unique NIR Spectra and Soil Signature?

Comparisons of the standardized greyscale values of both the placement and control samples indicate that CDIs do have a unique NIR spectra signature that can be differentiated from the surrounding soil. The significant difference between the standardized greyscale values of the control sites versus the true placement sites illustrates that the NIR spectra signatures of true CDIs is significantly different than that of the surrounding soil. This indicates that when viewed in the near-infrared spectrum, CDIs should be easily distinguishable from unaffected soils because true CDIs have dramatically higher NIR spectra signatures than that of the control sites. The visible difference in the chemical components between control sites and true placements further mirrors the above pattern (Table 3.1). The association between the strength of the NIR signature and the strength of the chemical composition of the soil demonstrates that the NIR methodology is only useful once purge has occurred, thereby introducing a concentration of organic chemicals into the soil. With the exception of C:N ratios, values for true placements are significantly higher for each variable than that of the controls, indicating not only that CDIs are significantly darker than unaffected soil in the NIR spectrum, but also that they contain significantly more organic material than unaffected soil. This stands to reason, as the NIR spectrum reflects and is affected by the amount of organic matter available (Ben-Dor et al. 1997; Kalacska and Bell 2006). The mean value for control placements (8.5 ± 1) is remarkably similar to that found by Aitkenhead-Peterson et al. (2012) in their decomposition study at the Southeast Texas Applied

Forensic Science facility in Huntsville, Texas. Interestingly, however, when examined individually the C:N ratios of true placements vary widely from very small values to very large, and do not universally approximate that of Aitkenhead-Peterson et al. (2012). No pattern was discovered when C:N ratios were compared to the data of true placements noted by the observers, indicating that a high C:N ratio is not necessarily indicative of a stronger NIR spectra signature, nor is a low C:N ratio indicative of a weaker signature. Further, there is not a strong correlation between C:N and the number of days that the cadaver has been in place. There is, however, a strong correlation between NPOC and TDN and the number of days in place, with the two chemical concentrations decreasing exponentially as time increases. The significantly higher values of NPOC and TDN in the true placements versus the controls and the strong correlation with time would indicate that the strength of the signature derives from these concentrations individually and from the length of time that the body has been in place, rather than from the ratio of the two chemicals.

How Long After Death Can CDIs Be Seen Using NIR?

Between approximately 700 and 800 days of placement, visibility of CDIs from the NIR aerial photographs decreases and the signature becomes indistinguishable from the surrounding soil (Figure 3.2). Beyond this time, CDIs may be visible only as near-white anomalies or may cease to be visible in the NIR spectrum altogether. CDIs that are younger than approximately 650 days old – but that are at least a week old – appear to have distinct visibility, with few exceptions, indicating that this span is the optimal period in which to discover human body placements utilizing this methodology. This is

consistent with the results of Parks (2011), who noted in her case study at FARF that rectal, oral, and aural purge began within the first week of decomposition.

There is a clear negative trend to the data that indicates that as the CDI ages, the strength of the NIR signature will fade (Figure 3.3). Therefore understanding how the CDIs will present in the NIR spectra over time is of the utmost importance. The presence of negative values – i.e., CDI areas that are significantly lighter in color than the surrounding soil – must be noted. In older placements, the extremely high organic content of the soil is utilized by opportunistic plant life. As a result, the reflectivity of the CDI in the NIR spectrum may over time move from extremely dark to near-white, as the vegetation absorbs and depletes the organic material. This near-white phenomenon is present between about 400 to 1000 days since placement (Figure 3.1). The effect of this progression is that older placements would be expected to have a negative SDV (much lighter than the surrounding soil) (Figure 4.1d) while more recent CDIs should have a high and positive standardized value (much darker than the surrounding soil) (Figure 4.1a). CDIs falling between these two extremes may simply have positive standardized values that are not as high as the most recent placements, or they may present as a dark circle surrounded by a very light ring (Figure 4.1b-c). This presentation would be indicative of a CDI that has vegetation growing around the edges. Interestingly, when the cadaver is still *in situ*, the anomaly may appear as a dark oval (the CDI) with a light center (the cadaver) (Figure 4.2).

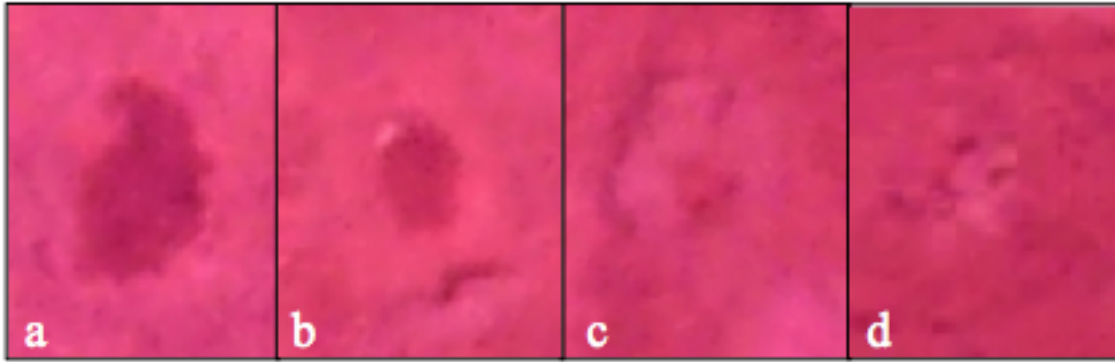


Figure 4.1. Examples illustrating the progression of CDI presentation types in the NIR spectrum. Image (a) represents the dark oval present in a recent CDI. Images (b) and (c) represent two possible presentations of the dark oval surrounded by a lighter ring. Image (d) represents the final stage in which the CDI is visible only as a very light oval.



Figure 4.2. Examples illustrating CDI reflectance when cadaver is *in situ*. Notice the light anomaly within the dark anomaly.

How Well Does Each Image Perform? Can People Successfully Find CDIs?

As mentioned previously, the two NIR surveys were taken using different exposure methods. The automatic exposure image produced an image with a pink shade, while the shutter priority produced an image with a blue shade (Figure 4.3). To test how well each exposure type performs, success rates were calculated for each individual and for each image (Table 3.2) based on the number of true placements that each individual correctly identified out of the total number of known placements visible in the image. For all three observers, performance was significantly higher when looking at the automatic exposure image than when looking at the shutter priority image, indicating that the automatic exposure method for taking NIR images is more effective when searching for clandestine human remains than is the shutter priority method. Because there are many more exposure methods available than just the two examined here, this creates a new research opportunity to examine all possible exposures to determine which allows for the most accurate and effective forensic searches.

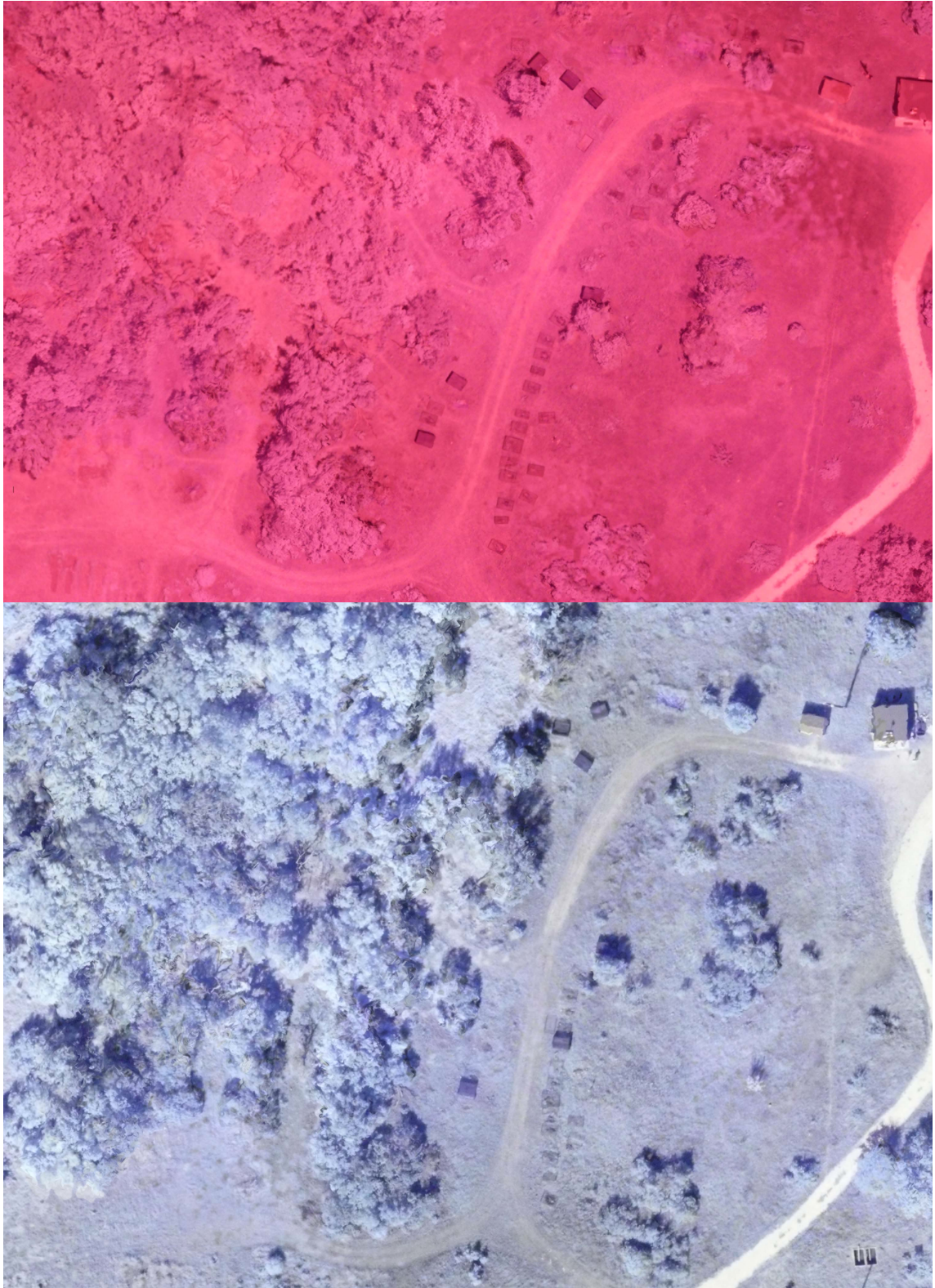


Figure 4.3. Images of FARF produced using automatic exposure (top) and shutter priority (bottom). Automatic exposure image taken on July 25th 2014 and shutter priority image taken on October 15th, 2014.

While the percentages in Table 3.2 discussed above provide an overall estimate of how successful each observer was at discovering CDIs from each image, it must be taken into consideration that some placements are significantly older than others. As mentioned above, after CDIs have been in place for more than 700 to 800 days (approximately 2 years), their signature fades and becomes nearly indistinguishable from the surrounding soil. Therefore, it is valuable to look at the success rates of each observer for each year that CDIs have been created at FARF. Consistent with the conclusions from the overall data, success rates were visibly higher in the automatic exposure image for every year, with the exception of 2009 where no placements were found in either image by any observer.

There is a visible pattern of success for the observers that decreases as CDIs increase in age. While each observer almost universally overlooked CDIs from 2009 to 2011, placements from 2014 had between an 84% - 100% success rate for two of the three examiners. This reinforces the conclusion from Figure 3.2 that CDIs younger than two years old show up much more vividly than those older than two years, which largely have faded to resemble the surrounding soil. As discussed above, not all CDIs will necessarily present with a dark oval, but might instead present as a near-white discoloration or as a dark oval with a white ring surrounding it. It is possible that, because the dark oval anomaly is the easiest to discern, the observers more commonly noted them rather than the lighter anomalies (which may not be so readily spotted). As a result, success rates increased where CDIs were most likely to show a darker anomaly (i.e., in more recent years). This possibility highlights the importance of training and experience for this methodology to be successful. While the observers were provided

instructions about what to look for, and were given an example to work from, they had no prior training in NIR imagery, and therefore likely missed anomalies that a seasoned researcher might have discovered. When this methodology is used in the search for clandestine remains, it is imperative that those observers searching the images for anomalies be trained to look for not only the dark anomalies, but also the near-white and intermediate anomalies, especially in cases where the individual has been missing for several years. It is also possible that since there were so many CDIs in a single area, the observers may simply have overlooked some anomalies that they might have detected had they only been searching for one or two sets of remains.

The discrepancy between the success rate of observer II versus that of observer I and III is interesting. Both observers I and II have some knowledge of FARF, though their degree of involvement in the placement of the cadavers varies from very little (individual II) to high (individual I). Observer III has no prior knowledge of where cadavers have been placed at FARF. None of the observers have used NIR imagery in any context prior to this study. It would seem to follow that observers I and II, who have prior knowledge of cadaver placements at the facility, would perform better than observer III, who has no prior knowledge. It is rather the case, however, that observers I and III strongly outperform observer II. Further, in all but one case, observer III was either more successful than or equally successful to observer I. It is possible that, in the case of observer II, the examiner's prior knowledge of the facility was in fact, a disadvantage rather than an advantage. Although instructed to circle all discovered anomalies, it is possible that certain CDIs (particularly those that were aligned in linear rows) may have been considered by the observer to be "too obvious" to note. Conversely, because

observer III had no prior knowledge of the facility (and therefore, no conception of what may be thought of as “obvious”), any anomaly would be seen as worthy of note as a potential CDI.

Alternatively, the discrepancy of observer II may be a result of differential selectivity. While observers I and III circled many anomalies and got many correct, there were also many anomalies circled that were not true CDIs. Though observer II only noted a few anomalies, they correctly identified most as true placements and had far fewer false positives. This scenario highlights another important consideration for searches for clandestine remains using this technology: selectivity. When this methodology is used in the field, standards of selection must be created so that the end product is useful, and not merely superfluous. Should an observer highlight a hundred potential anomalies in an area, this methodology may not be any more useful than a line search would be, as searchers will still have to search a large area of land on foot. Conversely, should an observer highlight only a few anomalies, there is a potential for missing the clandestine remains altogether. Although of course most search areas will not contain 100 or more sets of remains as the research facility does, it is important to bear in mind when using this technique that less is not always more, and more can sometimes be less. Future studies into the utility of this methodology should test the ability of observers to find only one or two CDIs in a large search area that is otherwise empty of remains.

**Do Animal Remains, Churned Soil, or Waterlogged Areas Present a Signature
Similar to CDIs?**

There is some indication that animal carcasses and churned soil, but not high moisture areas, may be mistaken for true human CDIs during aerial investigations. Two of the three observers noted the animal CDIs and false graves as anomalous. Animal carcasses present with a similar NIR reflectance signature to that of true CDIs and are therefore a potential confounding variable when this methodology is used in the field (SDV between 9 and 19 for automatic exposure and between 18 and 28 for shutter priority, cf. CDI values in Appendix D). This may become particularly problematic when the area being searched contains large animals (and therefore, potentially large CDIs), as would be the case in a ranch property or a farm. However, no other animal carcasses were noted on the property. It is possible that the four carcasses discovered by the observers were only visible in this instance because they were protected by cages and not permitted to be scavenged. Because many animal carcasses tend to be smaller than human bodies, scavengers can carry them off more easily, thereby diminishing the strength and concentration of the resulting CDI.

Although the false graves do not present with the same signature (i.e., darkness value) as true CDIs, it is clear from the responses of the testers that these areas of churned soil are visible in the NIR spectrum and may be mistaken for true CDIs during investigations. No observer noted the area of soil saturation created by the researcher, indicating that saturated soil areas do not present with an NIR signature similar to CDIs, and indeed, do not present with any signature unlike that of the unaffected soil. This

indicates that water saturation is not a potential confounding variable when searching for remains in the field.

Although the sample sizes for each of these variables is small, they do provide insights into potential issues governing the usage of NIR spectral imaging during the search for clandestine human remains. The most problematic of these issues appears to be the CDIs created by non-human animals, as these are the only confounding variable that present with an NIR signature very similar to that of humans when undisturbed by scavengers.

Does Seasonality Affect The Strength of the NIR Signature and the Amount of Organic Content in the Soil?

The MANOVA analysis run using Organic Content, NPOC, TDN, and SDV against Season (divided into two groups: Spring/Summer and Fall/Winter) does not indicate a significant difference between the seasons for any of the variables present. This contradicts previous studies, which do indicate a seasonal effect on both decomposition and the release of materials into the soil matrix, where warmer months show an increase in microbial and decomposition activity, and colder months show a dramatic decrease in these activities (Reed 1958; Rodriguez and Bass 1983; Vass et al. 1992). It is possible that the generally more temperate climate of central Texas – even during the Fall and Winter seasons – minimizes the effects of seasonality on human decomposition, and therefore on the creation of CDIs. Because seasonality could be a factor in areas where temperature does change more drastically, it will be important for future studies to take seasonality into consideration. The NIR spectra methodology may

be less effective on bodies placed in the Fall and Winter months in areas where colder temperatures may significantly slow the decomposition process.

Is the Signature Correlated with SOM, NPOC, or TDN?

There is a poor correlation between NIR signature and percentage of SOM and stronger correlations between the former and NPOC and TDN. Although the correlation is weak, there is a visual indication that as the percentage of SOM decreases, the NIR spectra signature correspondingly becomes weaker. It appears that once the percentage of SOM diminishes to between 5 and 15 percent, however, the correlation becomes erratic. There is a much stronger relationship between TDN and standardized greyscale value, indicating that TDN is a more appropriate predictor of the strength of a given NIR spectra signature. When a polynomial regression is applied to a scatterplot of NPOC, a fairly strong relationship between NIR signature strength and NPOC occurs ($R^2 = 0.48$). That a polynomial trendline best fits the scatter of standardized greyscale value against NPOC would indicate that organic carbon adequately predicts the strength of the NIR signature of a CDI until a peak level of organic carbon has been reached. Once this level (estimated to occur at about 5000 $\mu\text{g/g}$ of soil) has been surpassed, the total amount of organic carbon ceases to have a positive linear relationship with the strength of the NIR signature, and instead maintains a negative linear relationship.

Multiple linear regression analysis indicates that a combination of all three variables – organic content, organic carbon, and total nitrogen – provides a significantly better prediction of the strength of the NIR signature than does any single variable, with the exception of NPOC ($R^2 = .431$). Predictably, the correlation data indicate that NPOC

does individually account for the greatest explained variance in NIR signature, confirming that this variable contributes the most to the visibility of CDIs when using NIR cameras. It is further telling that BMI was eliminated during the stepwise calculations, as this indicates that BMI has no significant influence on the strength or weakness of the NIR signature. This conclusion is also mirrored in the univariate analyses of BMI and body weight, which showed no significant correlation between either BMI or body weight and any of the chemical variables examined. Interestingly, most discussions of cadaver decomposition point to cadaver size as a key factor in the size (both lateral and vertical) of the resulting CDI (Bohun et al. 2010; Carter et al. 2007; Towne 2000). It is possible that while body mass does affect the size and extent of the CDI (likely by determining how widely a scavenger can spread the remains), it does not equivalently affect the amount of organic material entering into the soil, or therefore, the strength of the NIR signature.

The second multiple linear regression analysis is perhaps even more telling, as it eliminates all variables from the analysis with the exception of TDN and Days Since Placement. When this equation is applied, 48.9% of the variation in NIR signature strength is explained and Days Since Placement individually accounts for the greatest explained variance. This illustrates not that organic compounds have less effect on NIR signature than the length of time that the CDI has been in place, but rather that the amount of organic material in the soil is highly dependent on the age of the CDI. As Benninger et al. (2008) discovered in their study, as PMI increases, the amount of nutrients in the soil decreases. It then follows that the strength of the organic material-dependent NIR signature would also decline as PMI increases.

These analyses indicate that while NPOC is the best single chemical predictor of the strength of the NIR signature, an understanding of the entire organic matrix of the soil as well as how this matrix depletes over time provides a much more accurate knowledge of when a CDI will cease to be visible in the near-infrared spectrum. Interestingly, Benninger et al. (2008) note no correlation between total carbon and PMI, with control soil and gravesoil exhibiting similar fluctuations in content. In tandem with the results presented here, this would appear to indicate that organic carbon, rather than total carbon, is more useful in discussions of PMI.

Although only organic carbon and nitrogen have been explored in this study, there are undoubtedly other materials that contribute to the strength or weakness of the signature that ought to be explored in future studies.

Experimental Design

It is clear from the results of the present study that there are strengths and weaknesses to every experimental design. Equivalently, there are arguments for and against the various methods by which an outdoor decomposition facility such as the one employed for this research may be organized. Because the earliest donations were laid out seemingly at random without an easily-recognized pattern, it was much more difficult for my colleague and I to discover where cadavers had been placed, and therefore many of the older placements were regrettably excluded from the analysis. The non-linear organization of these earlier placements, however, did allow for a more realistic scenario when volunteers were asked to search for and indicate potential CDIs. Conversely, the linear organization of many of the recent placements, while enabling the researchers to

discover and map more donations, did have the adverse effect of making the CDIs “too obvious” for the volunteers. In a real world scenario, it is unlikely that clandestine human remains will be laid out so precisely.

An additional point of interest in this research is the use of the eyedropper tool in Adobe Photoshop® as a means of sampling for NIR signature strength. While there are other means of calculating NIR signatures and comparing these to control sites, they require data and instrumentation that was not available for this study. For example, Kalacska et al. (2009) utilized wavelength and reflectance data to graphically determine whether a mass grave could be differentiated from a control site using hyperspectral remote imagery. However, gathering this data required the cooperation of an outside corporation that had the software to produce this data. Similarly, there are formulae that can determine how similar or dissimilar two spectral signatures are in amplitude and shape, however these also require wavelength data that was unavailable in this study (Price 1994; Snirer 2013). The use of the eyedropper tool was the most efficient and cost-effective means of estimating NIR spectra signature strength in a uniform and accurate way.

Conclusions

For vast areas where searching for a body would otherwise be like searching for a needle in a haystack, NIR imaging is an extremely viable and worthwhile process. It requires a much smaller search team, takes considerably less time, and is much safer for all involved. Further, not only does this methodology work when the cadaver is still *in situ*, it is also effective even when the body is no longer still associated with the CDI.

Should this be the case, investigators can then use the CDI as a starting location to begin the search for associated remains. This method facilitates the search process by allowing law enforcement, forensic anthropologists, and other participants to narrow down the search area by pinpointing a few select anomalies. In so doing, investigators will be able to target key areas to search more thoroughly and with fewer people, rather than wasting time, energy, and money having to search a large area that may or may not contain human remains. Further, volunteers will not be forced to walk over potentially dangerous terrain where snakes, poison plants, and other dangers might be hidden to seek out remains.

The recent controversy surrounding drones and their usage, particularly for commercial purposes, does create a problematic environment for the usage of this methodology. As of 2007, drone operators – even those who utilize their technology for search and rescue efforts – cannot legally fly UAS commercially without permission from the Federal Aviation Administration (FAA 2014). Further, drones cannot be flown over private property without express permission from the property owners. Certain drone flight companies have discovered ways to bypass at least the first of these issues by obtaining special research certificates for testing the machines, for example, or by registering their operation as a nonprofit organization (Francescani 2013). Despite these efforts, however, the restrictions on drone technology can still present a problem, particularly for forensic investigators who cannot afford to lose the time required to request, process, and receive the FAA permits (FAA 2014; Francescani 2013). In these emergency situations, some UAS pilots have found that “it [is] going to be easier to ask forgiveness than permission” (Francescani 2013).

While this study has demonstrated that there are several potential problems with this methodology, most of these can be solved by proper training and experience. If searchers are provided with examples of the three main CDI presentation types – dark, near-white, and dark encircled with near-white – as references and are given training by experts seasoned in the use of NIR imaging, a higher rate of success can be achieved. False anomalies such as churned earth may also be eliminated from the search in this way. The two most important pitfalls of this methodology are animal decomposition and tree cover. Currently, there is no good way to distinguish animal CDIs from human CDIs in a NIR image: the signatures are nearly identical, and the smaller size of animals is equivalent to the shrinking CDIs of some older placements. This dilemma will be a key question for future studies. Tree cover is also problematic as the near-infrared photography captures only surface reflectance. The reflectance from the leaf litter of the trees therefore interrupts the NIR signature and makes identifying CDIs that might lie beneath the canopy impossible. It is possible that a different exposure method for the images may be able to eliminate the distortion from the trees, but as of this study it is unlikely that NIR cameras mounted on UAS will be a viable search method for heavily treed areas. For this reason, this method will be primarily effective in open country, and not very effective in more forested areas. However, this methodology could be an incredibly effective tool for the Department of Homeland Security to utilize in the humanitarian crisis along the US-Mexico border in Texas and Arizona. Because so many individuals die attempting to cross the border in these areas, NIR technology mounted to UAS could greatly facilitate the search for and the repatriation of these missing individuals.

This study has demonstrated that NIR imaging and drone technology will provide a fast, safe, and effective means of searching for clandestine remains that was not available in the past. This methodology is particularly successful for clandestine remains that have been in place for at least a week but less than two years, particularly when using the automatic exposure technique for producing the images. Though there are problems with this technique, many may be examined and nullified with just a few short years of research, particularly into the different exposure methods. Should law enforcement embrace UAS technology and NIR imaging as a method of search and recovery, it will streamline a process that once took days or even weeks and will bring answers to missing persons cases that might otherwise have been unsolved forever.

APPENDIX SECTION

APPENDIX A

Donation Numbers and Date of Placement

Donation #	Date of Surface Placement
D10-2009	11/19/09
D20-2011	11/28/11
D21-2011	11/30/11
D22-2011	12/5/11
D03-2012	1/28/12
D04-2012	1/28/12
D06-2012	2/13/12
D10-2012	3/30/12
D11-2012	3/30/12
D13-2012	4/26/12
D14-2012	4/30/12
D16-2012	5/9/12
D19-2012	5/23/12
D24-2012	6/21/12
D27-2012	7/14/12
D29-2012	7/13/12
D30-2012	7/27/12
D31-2012	7/27/12
D33-2012	9/13/12
D34-2012	8/31/12
D35-2012	9/6/12
D36-2012	9/14/12
D38-2012	10/18/12
D41-2012	10/31/12
D42-2012	11/3/12
D43-2012	11/3/12
D44-2012	11/9/12
D46-2012	11/30/12
D47-2012	12/9/12
D48-2012	12/12/12
D49-2012	12/18/12
D50-2012	1/1/13
D02-2013	1/18/13
D03-2013	1/18/13

Donation #	Date of Surface Placement
D05-2013	1/28/13
D06-2013	1/26/13
D07-2013	1/28/13
D08-2013	2/1/13
D11-2013	2/11/13
D13-2013	2/18/13
D14-2013	2/19/13
D15-2013	2/27/13
D16-2013	2/27/13
D17-2013	4/5/13
D19-2013	4/5/13
D20-2013	4/19/13
D22-2013	4/26/13
D23-2013	5/6/13
D24-2013	5/7/13
D26-2013	6/3/13
D28-2013	6/9/13
D29-2013	6/14/13
D30-2013	6/21/13
D31-2013	6/25/13
D33-2013	7/3/13
D34-2013	7/5/13
D35-2013	7/9/13
D36-2013	7/15/13
D39-2013	7/18/13
D46-2013	8/13/13
D47-2013	8/12/13
D50-2013	9/21/13
D51-2013	9/22/13
D52-2013	9/27/13
D54-2013	10/11/13
D56-2013	10/22/13
D57-2013	10/19/13
D59-2013	11/1/13
D61-2013	11/7/13
D65-2013	11/21/13
D01-2014	1/10/14
D02-2014	1/30/14
D03-2014	1/30/14

Donation #	Date of Surface Placement
D04-2014	2/11/14
D05-2014	2/14/14
D06-2014	2/10/14
D07-2014	2/14/14
D08-2014	2/18/14
D09-2014	2/28/14
D10-2014	2/28/14
D11-2014	3/19/14
D12-2014	3/5/14
D13-2014	3/10/14
D14-2014	3/10/14
D15-2014	3/19/14
D16-2014	3/14/14
D17-2014	4/3/14
D19-2014	4/11/14
D20-2014	4/15/14
D21-2014	4/29/14
D23-2014	6/6/14
D24-2014	6/8/14
D25-2014	5/21/14
D26-2014	6/6/14
D27-2014	6/18/14
D28-2014	6/27/14
D29-2014	6/24/14
D30-2014	6/23/14
D32-2014	6/26/14
D33-2014	6/30/14
D35-2014	7/15/14
D36-2014	7/15/14
D37-2014	7/23/14

APPENDIX B

Ash-Free Dry Weight Analysis Data

Donation #	Mass of Crucible (g)	Mass of Crucible + Soil Before Kiln (g)	Mass of Crucible + Soil After Kiln (g)	Mass of Dry Soil (g)	Mass of Ashed Soil (g)	Mass of Organic Matter (g)	Organic Content (%)
D10-2009	18.540	34.749	32.984	16.209	14.444	1.765	10.88901228
D20-2011	15.922	36.368	34.273	20.446	18.351	2.095	10.24650298
D21-2011	17.945	38.572	36.082	20.627	18.137	2.490	12.0715567
D22-2011	17.016	38.264	35.982	21.248	18.966	2.282	10.73983434
D03-2012	15.925	42.022	39.552	26.097	23.627	2.470	9.464689428
D04-2012	18.49	43.724	41.229	25.234	22.739	2.495	9.887453436
D06-2012	15.924	39.637	38.094	23.713	22.170	1.543	6.506979294
D10-2012	17.944	45.744	44.151	27.800	26.207	1.593	5.730215827
D11-2012	15.922	32.796	31.212	16.874	15.290	1.584	9.387222947
D13-2012	16.743	38.896	37.282	22.153	20.539	1.614	7.28569494
D14-2012	17.018	39.616	37.195	22.598	20.177	2.421	10.71333746
D16-2012	17.943	40.691	38.406	22.748	20.463	2.285	10.04483911
D19-2012	18.543	38.901	37.379	20.358	18.836	1.522	7.476176442
D24-2012	16.743	40.722	38.225	23.979	21.482	2.497	10.41327829
D27-2012	18.541	42.059	39.417	23.518	20.876	2.642	11.23394847
D29-2012	18.851	38.686	36.205	19.835	17.354	2.481	12.50819259
D30-2012	18.847	36.239	34.935	17.392	16.088	1.304	7.497700092
D31-2012	16.743	43.402	41.324	26.659	24.581	2.078	7.794740988
D33-2012	18.495	41.664	39.445	23.169	20.950	2.219	9.577452631

Donation #	Mass of Crucible (g)	Mass of Crucible + Soil Before Kiln (g)	Mass of Crucible + Soil After Kiln (g)	Mass of Dry Soil (g)	Mass of Ashed Soil (g)	Mass of Organic Matter (g)	Organic Content (%)
D34-2012	18.542	43.323	41.411	24.781	22.869	1.912	7.715588556
D35-2012	18.846	45.43	43.23	26.584	24.384	2.200	8.275654529
D36-2012	17.126	50.863	47.299	33.737	30.173	3.564	10.56406912
D38-2012	18.851	37.757	36.629	18.906	17.778	1.128	5.966359886
D41-2012	18.852	39.536	37.491	20.684	18.639	2.045	9.886869078
D42-2012	17.126	40.142	37.952	23.016	20.826	2.190	9.515119917
D43-2012	18.851	39.91	38	21.059	19.149	1.910	9.069756399
D44-2012	18.487	43.024	40.343	24.537	21.856	2.681	10.92635612
D46-2012	18.487	38.331	35.713	19.844	17.226	2.618	13.19290466
D47-2012	17.944	34.866	31.706	16.922	13.762	3.160	18.67391561
D48-2012	17.018	42.478	39.238	25.460	22.220	3.240	12.72584446
D49-2012	18.853	37.71	34.706	18.857	15.853	3.004	15.93042372
D50-2012	18.54	28.311	27.412	9.771	8.872	0.899	9.200695937
D02-2013	16.744	29.212	28.161	12.468	11.417	1.051	8.429579724
D03-2013	17.945	31.956	30.144	14.011	12.199	1.812	12.93269574
D05-2013	18.851	43.587	40.786	24.736	21.935	2.801	11.32357697
D06-2013	17.126	41.806	39.362	24.680	22.236	2.444	9.902755267
D07-2013	18.847	41.939	39.318	23.092	20.471	2.621	11.35025117
D08-2013	16.744	34.155	32.075	17.411	15.331	2.080	11.94647062
D11-2013	18.848	39.561	37.531	20.713	18.683	2.030	9.800608314
D13-2013	15.924	42.913	39.458	26.989	23.534	3.455	12.80151173
D14-2013	17.944	40.581	37.093	22.637	19.149	3.488	15.40840217

Donation #	Mass of Crucible (g)	Mass of Crucible + Soil Before Kiln (g)	Mass of Crucible + Soil After Kiln (g)	Mass of Dry Soil (g)	Mass of Ashed Soil (g)	Mass of Organic Matter (g)	Organic Content (%)
D15-2013	18.851	38.152	36.864	19.301	18.013	1.288	6.673229366
D16-2013	18.488	46.431	43.718	27.943	25.230	2.713	9.709050567
D17-2013	18.541	49.201	46.889	30.660	28.348	2.312	7.540769733
D19-2013	18.488	51.8	48.823	33.312	30.335	2.977	8.9367195
D20-2013	17.944	52.914	49.337	34.970	31.393	3.577	10.22876752
D22-2013	18.852	48.544	45.92	29.692	27.068	2.624	8.837397279
D23-2013	17.02	40.134	36.977	23.114	19.957	3.157	13.65838886
D24-2013	18.54	47.539	45.619	28.999	27.079	1.920	6.620917963
D26-2013	15.923	35.737	32.663	19.814	16.740	3.074	15.51428283
D28-2013	15.922	32.722	31.807	16.800	15.885	0.915	5.446428571
D29-2013	17.018	40.488	38.741	23.470	21.723	1.747	7.443544951
D30-2013	18.847	39.627	38.235	20.780	19.388	1.392	6.698748797
D31-2013	17.126	40.846	37.676	23.720	20.550	3.170	13.36424958
D33-2013	16.746	41.88	39.496	25.134	22.750	2.384	9.485159545
D34-2013	17.02	44.644	41.884	27.624	24.864	2.760	9.991311903
D35-2013	17.126	39.822	38.359	22.696	21.233	1.463	6.446069792
D36-2013	18.488	47.165	44.78	28.677	26.292	2.385	8.316769537
D39-2013	17.128	45.831	42.971	28.703	25.843	2.860	9.964115249
D46-2013	16.743	42.003	38.421	25.260	21.678	3.582	14.18052257
D47-2013	16.745	38.82	36.414	22.075	19.669	2.406	10.89920725
D50-2013	17.016	43.762	41.451	26.746	24.435	2.311	8.64054438
D51-2013	18.848	46.663	43.703	27.815	24.855	2.960	10.64174007

Donation #	Mass of Crucible (g)	Mass of Crucible + Soil Before Kiln (g)	Mass of Crucible + Soil After Kiln (g)	Mass of Dry Soil (g)	Mass of Ashed Soil (g)	Mass of Organic Matter (g)	Organic Content (%)
D52-2013	16.745	36.433	32.316	19.688	15.571	4.117	20.91121495
D54-2013	17.126	36.984	35.414	19.858	18.288	1.570	7.906133548
D56-2013	18.54	43.922	41.865	25.382	23.325	2.057	8.104168308
D57-2013	18.487	36.36	34.31	17.873	15.823	2.050	11.4698148
D59-2013	18.847	45.175	42.325	26.328	23.478	2.850	10.82497721
D61-2013	17.945	46.363	43.659	28.418	25.714	2.704	9.515096066
D65-2013	16.744	44.388	41.025	27.644	24.281	3.363	12.16538851
D01-2014	18.488	45.715	40.649	27.227	22.161	5.066	18.60653028
D02-2014	18.848	39.678	36.594	20.830	17.746	3.084	14.80556889
D03-2014	18.54	43.425	37.898	24.885	19.358	5.527	22.21016677
D04-2014	18.852	44.597	40.388	25.745	21.536	4.209	16.34880559
D05-2014	15.922	35.784	33.856	19.862	17.934	1.928	9.706978149
D06-2014	17.018	39.195	35.553	22.177	18.535	3.642	16.42241962
D07-2014	18.85	40.468	35.469	21.618	16.619	4.999	23.12424831
D08-2014	16.744	48.251	43.534	31.507	26.790	4.717	14.97127622
D09-2014	20.664	35.985	34.859	15.321	14.195	1.126	7.349389727
D10-2014	18.488	34.582	30.72	16.094	12.232	3.862	23.99652044
D12-2014	18.851	48.096	44.98	29.245	26.129	3.116	10.65481279
D13-2014	18.848	44.891	42.789	26.043	23.941	2.102	8.071266751
D14-2014	17.018	42.74	36.95	25.722	19.932	5.790	22.50991369
D15-2014	17.126	49.981	44.24	32.855	27.114	5.741	17.47374829
D16-2014	17.945	41.767	36.398	23.822	18.453	5.369	22.53799009

Donation #	Mass of Crucible (g)	Mass of Crucible + Soil Before Kiln (g)	Mass of Crucible + Soil After Kiln (g)	Mass of Dry Soil (g)	Mass of Ashed Soil (g)	Mass of Organic Matter (g)	Organic Content (%)
D17-2014	17.126	39.343	33.604	22.217	16.478	5.739	25.83157042
D19-2014	15.925	44.464	41.848	28.539	25.923	2.616	9.166403868
D20-2014	17.02	40.982	36.629	23.962	19.609	4.353	18.16626325
D20-2014	15.923	35.471	31.305	19.548	15.382	4.166	21.31164313
D21-2014	18.54	43.644	37.926	25.104	19.386	5.718	22.77724665
D23-2014	18.539	41.602	38.354	23.063	19.815	3.248	14.08316351
D24-2014	18.49	39.427	34.959	20.937	16.469	4.468	21.34021111
D25-2014	17.126	41.843	36.401	24.717	19.275	5.442	22.0172351
D26-2014	20.664	51.478	47.977	30.814	27.313	3.501	11.3617187
D27-2014	20.664	46.5	39.579	25.836	18.915	6.921	26.78820251
D28-2014	18.54	35.282	27.199	16.742	8.659	8.083	48.27977542
D29-2014	20.664	53.464	48.537	32.800	27.873	4.927	15.02134146
D30-2014	17.126	50.789	47.464	33.663	30.338	3.325	9.877313371
D32-2014	17.946	51.576	47.409	33.630	29.463	4.167	12.39072257
D33-2014	16.745	39.469	33.866	22.724	17.121	5.603	24.65675057
D35-2014	17.127	41.288	36.099	24.161	18.972	5.189	21.47676007
D36-2014	15.922	47.746	42.109	31.824	26.187	5.637	17.71304676
D37-2014	17.019	36.996	32.943	19.977	15.924	4.053	20.28833158
N1	18.848	42.568	41.044	23.720	22.196	1.524	6.424957841
N2	15.921	39.476	37.633	23.555	21.712	1.843	7.824241138
N3	15.922	42.019	39.115	26.097	23.193	2.904	11.12771583
N4	17.018	47.111	45.228	30.093	28.210	1.883	6.257269132

Donation #	Mass of Crucible (g)	Mass of Crucible + Soil Before Kiln (g)	Mass of Crucible + Soil After Kiln (g)	Mass of Dry Soil (g)	Mass of Ashed Soil (g)	Mass of Organic Matter (g)	Organic Content (%)
N5	18.848	47.219	45.184	28.371	26.336	2.035	7.172817313
N6	18.853	47.725	45.969	28.872	27.116	1.756	6.082017179
T1	17.017	53.741	50.965	36.724	33.948	2.776	7.559089424
T2	16.744	35.183	33.089	18.439	16.345	2.094	11.35636423
T3	18.541	44.776	42.011	26.235	23.470	2.765	10.53935582
T4	18.489	34.193	32.502	15.704	14.013	1.691	10.76795721
T5	17.128	35.475	33.939	18.347	16.811	1.536	8.371940917
T6	20.664	49.556	46.256	28.892	25.592	3.300	11.42184688

APPENDIX C

Chemical Analysis (NPOC and TDN) Data

	ug/g soil		
Donation #	NPOC	TDN	C:N
D10-2009	294.36	24.27	12.1
D20-2011	344.72	42.19	8.2
D21-2011	782.18	53.72	14.6
D22-2011(?)	606.16	44.76	13.5
D03-2012	658.61	74.15	8.9
D04-2012	531.42	50.43	10.5
D06-2012	453.08	40.48	11.2
D10-2012	374.70	31.29	12.0
D13-2012	935.79	175.58	5.3
D14-2012	869.74	67.91	12.8
D16-2012	894.74	282.26	3.2
D19-2012	596.50	87.07	6.9
D27-2012	903.05	143.46	6.3
D29-2012	443.65	55.28	8.0
D30-2012	1651.06	242.61	6.8
D31-2012	647.58	71.72	9.0
D33-2012	621.28	59.19	10.5
D34-2012	829.64	170.91	4.9
D35-2012	615.54	49.10	12.5
D36-2012	989.84	111.60	8.9
D38-2012	393.03	35.48	11.1
D41-2012	664.88	78.66	8.5
D43-2012	1141.90	105.16	10.9
D46-2012	2560.09	459.34	5.6
D48-2012	421.26	84.83	5.0
D03-2013	594.28	96.74	6.1
D06-2013	481.26	875.08	0.5
D07-2013	2660.56	595.09	4.5
D08-2013	477.75	264.19	1.8
D11-2013	645.34	173.80	3.7
D13-2013	1238.31	510.98	2.4
D14-2013	6066.98	390.45	15.5
D15-2013	1311.89	154.96	8.5
D16-2013	5750.39	692.05	8.3

	ug/g soil		
Donation #	NPOC	TDN	C:N
D17-2013	495.98	97.68	5.1
D19-2013	1132.84	592.00	1.9
D20-2013	774.83	70.08	11.1
D22-2013	1061.98	309.17	3.4
D23-2013	3941.45	933.54	4.2
D24-2013	677.41	157.16	4.3
D26-2013	633.85	418.84	1.5
D29-2013	655.87	62.10	10.6
D30-2013	822.45	135.56	6.1
D31-2013	1487.27	574.83	2.6
D33-2013	942.91	150.61	6.3
D36-2013	1022.26	135.27	7.6
D46-2013	2434.67	460.22	5.3
D47-2013	5342.91	230.35	23.2
D50-2013	2743.69	126.06	21.8
D52-2013	6661.49	311.06	21.4
D54-2013	1243.00	552.86	2.2
D56-2013	736.66	281.83	2.6
D61-2013	2412.56	610.03	4.0
D65-2013	760.63	478.43	1.6
D01-2014	9822.39	216.22	45.4
D02-2014	6577.41	327.46	20.1
D03-2014	6191.98	177.64	34.9
D04-2014	7516.00	430.81	17.4
D05-2014	736.61	170.27	4.3
D06-2014	8343.49	159.33	52.4
D07-2014	6831.48	360.00	19.0
D08-2014	3090.29	842.81	3.7
D09-2014	1009.19	339.50	3.0
D10-2014	8233.08	399.00	20.6
D11-2014	8413.91	212.82	39.5
D12-2014	4580.96	256.06	17.9
D13-2014	1016.12	479.09	2.1
D14-2014	6063.22	981.00	6.2
D15-2014	6805.52	478.13	14.2
D16-2014	7934.60	1042.65	7.6
D17-2014	6573.19	984.06	6.7
D19-2014	2749.34	116.10	23.7

	ug/g soil		
Donation #	NPOC	TDN	C:N
D20-2014	4752.95	624.65	7.6
D21-2014	6992.93	1429.53	4.9
D24-2014	4447.14	1245.04	3.6
D25-2014	7530.65	323.94	23.2
D27-2014	10111.47	551.90	18.3
D28-2014	5876.57	119.77	49.1
D29-2014	5347.48	513.23	10.4
D32-2014	5476.43	930.20	5.9
D33-2014	8874.98	536.52	16.5
D35-2014	15806.24	541.07	29.2
D36-2014	2862.51	66.04	43.3
D37-2014	5762.99	99.33	58.0
N1	223.01	27.44	8.1
N2	240.68	28.50	8.4
N3	392.09	41.03	9.6
N4	236.89	28.41	8.3
N5	278.05	32.08	8.7
N6	279.42	42.52	6.6
T1	192.90	24.75	7.8
T2	346.39	31.98	10.8
T3	275.76	33.62	8.2
T4	286.87	34.10	8.4
T5	319.17	36.93	8.6
T6	286.30	35.83	8.0

APPENDIX D

NIR Standardized Darkness Value Data

	FLYOVER 1								
Donation #	1	2	3	4	5	Average	5x5	Perimeter	SDV (x-y=z)
D10-2009	51	50	51	49	51	50.4	51	52	-1
D20-2011	47	45	44	47	48	46.2	47	50	-3
D21-2011	45	46	47	45	44	45.4	45	48	-3
D22-2011	44	46	41	43	45	43.8	46	48	-2
D03-2012	48	51	50	47	49	49	48	50	-2
D04-2012	41	42	40	42	40	41	41	40	1
D06-2012	52	53	50	47	49	50.2	50	49	1
D10-2012	42	41	40	41	42	41.2	41	40	1
D11-2012						0			
D13-2012	49	50	49	49	51	49.6	49	49	0
D14-2012	47	47	45	45	46	46	46	46	0
D16-2012	59	58	57	51	59	56.8	57	48	9
D19-2012	51	53	56	54	52	53.2	54	53	1
D24-2012	49	50	49	50	52	50	50	47	3
D27-2012	54	49	51	52	51	51.4	51	49	2
D29-2012	51	53	49	50	49	50.4	51	50	1
D30-2012	45	44	45	45	44	44.6	45	44	1
D31-2012	46	46	45	46	47	46	46	49	-3
D33-2012						0			
D34-2012	49	51	50	52	52	50.8	50	49	1
D35-2012	50	46	45	49	47	47.4	48	48	0

Donation #	FLYOVER 1							Perimeter	SDV (x-y=z)
	1	2	3	4	5	Average	5x5		
D36-2012	TARPED CAGE								0
D38-2012	54	52	53	56	53	53.6	54	48	6
D41-2012	51	56	52	50	54	52.6	53	50	3
D42-2012	54	55	54	51	55	53.8	54	45	9
D43-2012	50	49	49	50	50	49.6	49	49	0
D44-2012	55	53	56	57	54	55	54	44	10
D46-2012	51	49	51	50	50	50.2	49	49	0
D47-2012						0			
D48-2012	49	53	52	52	53	51.8	51	52	-1
D49-2012	56	58	60	53	54	56.2	55	48	7
D50-2012	51	49	48	50	52	50	50	53	-3
D02-2013	51	49	49	50	49	49.6	50	50	0
D03-2013	49	50	51	50	49	49.8	50	48	2
D05-2013	53	52	48	50	51	50.8	52	51	1
D06-2013	56	55	55	54	53	54.6	53	43	10
D07-2013	55	56	50	54	54	53.8	54	48	6
D08-2013	43	46	45	43	45	44.4	45	46	-1
D11-2013	51	48	49	50	52	50	51	51	0
D13-2013	61	62	63	64	61	62.2	60	55	5
D14-2013	TARPED CAGE								
D15-2013	57	55	56	57	56	56.2	56	48	8
D16-2013	60	61	60	61	59	60.2	60	48	12
D17-2013	51	52	55	51	52	52.2	52	55	-3
D19-2013	52	55	54	54	55	54	55	51	4

	FLYOVER 1								
Donation #	1	2	3	4	5	Average	5x5	Perimeter	SDV (x-y=z)
D20-2013	52	56	54	52	54	53.6	55	58	-3
D22-2013	47	51	48	49	49	48.8	49	50	-1
D23-2013	UNDER TARP??								
D24-2013	52	51	52	51	53	51.8	51	49	2
D26-2013	52	53	52	54	53	52.8	53	46	7
D28-2013	48	49	48	48	47	48	48	48	0
D29-2013	51	49	50	47	48	49	49	45	4
D30-2013	50	48	49	50	50	49.4	50	49	1
D31-2013	57	56	56	58	55	56.4	57	46	11
D33-2013	56	57	55	51	52	54.2	55	50	5
D34-2013	51	50	51	51	52	51	51	46	5
D35-2013	59	54	54	57	55	55.8	57	49	8
D36-2013	TARPED CAGE								
D39-2013	42	42	41	40	41	41.2	42	47	-5
D46-2013	53	57	55	55	56	55.2	56	44	12
D47-2013	57	61	58	59	56	58.2	57	46	11
D50-2013	69	63	65	66	68	66.2	67	47	20
D51-2013	66	61	63	67	65	64.4	66	53	13
D52-2013	TARPED CAGE								
D54-2013	54	50	50	52	53	51.8	52	46	6
D56-2013	50	52	49	53	50	50.8	50	42	8
D57-2013	TARPED CAGE								
D59-2013	54	52	55	52	54	53.4	53	45	8
D61-2013	54	51	50	50	51	51.2	51	44	7

Donation #	FLYOVER 1							Perimeter	SDV (x-y=z)
	1	2	3	4	5	Average	5x5		
D65-2013	TARPED CAGE								
D01-2014	TARPED CAGE								
D02-2014	61	55	61	56	60	58.6	58	48	10
D03-2014	59	57	58	56	50	56	56	48	8
D04-2014	60	58	57	56	60	58.2	57	49	8
D05-2014	59	61	56	61	56	58.6	57	48	9
D06-2014	61	63	60	61	63	61.6	61	55	6
D07-2014	62	54	56	61	58	58.2	58	49	9
D08-2014	58	57	54	55	57	56.2	56	50	6
D09-2014	58	55	56	58	56	56.6	57	50	7
D10-2014	58	60	57	57	58	58	58	50	8
D11-2014	63	55	59	56	58	58.2	58	50	8
D12-2014	60	60	56	61	55	58.4	58	50	8
D13-2014	56	54	56	57	56	55.8	56	47	9
D14-2014	59	63	60	62	61	61	61	49	12
D15-2014	61	57	53	58	58	57.4	58	48	10
D16-2014	62	49	60	56	55	56.4	56	49	7
D17-2014	64	61	58	66	59	61.6	61	49	12
D19-2014	62	55	59	59	63	59.6	59	46	13
D20-2014	56	54	58	55	57	56	57	49	8
D21-2014	58	57	61	58	59	58.6	58	49	9
D23-2014						0			
D24-2014						0			
D25-2014						0			

	FLYOVER 1								
Donation #	1	2	3	4	5	Average	5x5	Perimeter	SDV (x-y=z)
D26-2014						0			
D27-2014						0			
D28-2014						0			
D29-2014	56	58	60	58	62	58.8	57	50	7
D30-2014						0			
D32-2014	55	62	60	59	56	58.4	58	47	11
D33-2014						0			
D35-2014						0			
D36-2014						0			
D37-2014						0			
N1						0	50	51	-1
N2						0	50	49	1
N3						0	48	48	0
N4						0	49	49	0
N5						0	47	48	-1
N6						0	50	50	0
T1						0	44	43	1
T2						0	43	42	1
T3						0	42	43	-1
T4						0	45	44	1
T5						0	43	43	0
T6						0	42	41	1

FLYOVER 2

Donation #	1	2	3	4	5	Average	5x5	Perimeter	x-y=z
D10-2009	29	26	32	29	30	29.2	27	28	-1
D20-2011	23	18	19	17	21	19.6	22	19	3
D21-2011						0			
D22-2011	28	26	26	26	27	26.6	28	30	-2
D03-2012	40	35	41	34	36	37.2	37	36	1
D04-2012						0			
D06-2012	36	35	38	36	35	36	36	34	2
D10-2012						0			
D11-2012						0			
D13-2012	35	34	31	35	33	33.6	31	31	0
D14-2012						0			
D16-2012	51	56	50	55	53	53	55		55
D19-2012	41	37	38	39	41	39.2	39	32	7
D24-2012	59	55	58	61	56	57.8	58	31	27
D27-2012	38	37	40	33	36	36.8	36	25	11
D29-2012	58	49	54	56	58	55	56	27	29
D30-2012	37	36	35	38	38	36.8	36	32	4
D31-2012	30	31	30	27	30	29.6	30	34	-4
D33-2012						0			
D34-2012	33	39	34	35	34	35	36	41	-5
D35-2012	32	30	30	32	31	31	32		32
D36-2012	43	48	50	43	44	45.6	47	31	16
D38-2012	35	33	34	32	34	33.6	33	31	2
D41-2012	20	24	21	21	20	21.2	23	20	3
D42-2012	46	44	44	49	45	45.6	46	31	15

	FLYOVER 2								
Donation #	1	2	3	4	5	Average	5x5	Perimeter	x-y=z
D43-2012						0			
D44-2012	53	47	51	49	44	48.8	51	31	20
D46-2012	39	43	39	46	43	42	42	29	13
D47-2012						0			
D48-2012	43	32	34	33	41	36.6	37	35	2
D49-2012	53	50	49	51	54	51.4	51	30	21
D50-2012	46	42	47	40	45	44	45	27	18
D02-2013	39	37	36	38	36	37.2	38	35	3
D03-2013	30	25	31	29	32	29.4	32	37	-5
D05-2013	35	42	38	39	40	38.8	41	28	13
D06-2013						0			
D07-2013	51	41	42	51	43	45.6	45	33	12
D08-2013	34	36	37	34	38	35.8	35		35
D11-2013	44	43	42	40	44	42.6	44	26	18
D13-2013	58	56	50	51	57	54.4	57	25	32
D14-2013	43	40	43	43	40	41.8	41	28	13
D15-2013	38	37	36	36	37	36.8	36	38	-2
D16-2013	54	57	50	54	54	53.8	54	31	23
D17-2013	25	27	28	29	30	27.8	28	26	2
D19-2013	38	46	39	42	38	40.6	39	27	12
D20-2013	38	45	42	41	45	42.2	40	36	4
D22-2013						0			
D23-2013	UNDER TARP??								
D24-2013	30	29	28	27	30	28.8	29	22	7
D26-2013	33	33	32	31	32	32.2	31	39	-8

	FLYOVER 2								
Donation #	1	2	3	4	5	Average	5x5	Perimeter	x-y=z
D28-2013	34	33	33	34	33	33.4	33	28	5
D29-2013	40	44	37	44	42	41.4	43	26	17
D30-2013	32	36	34	38	37	35.4	34	33	1
D31-2013	52	51	48	46	48	49	49	28	21
D33-2013	29	31	33	29	32	30.8	29	41	-12
D34-2013	49	46	44	48	51	47.6	45	31	14
D35-2013	42	41	44	40	41	41.6	41	30	11
D36-2013	45	42	41	44	43	43	44	33	11
D39-2013	16	18	17	13	15	15.8	16	26	-10
D46-2013	60	65	57	55	56	58.6	61	27	34
D47-2013	47	44	45	45	44	45	45	30	15
D50-2013	54	62	57	63	61	59.4	61	31	30
D51-2013	51	52	49	50	48	50	50	32	18
D52-2013	TARPED CAGE								
D54-2013	49	52	50	51	54	51.2	52	36	16
D56-2013						0			
D57-2013						0			
D59-2013	51	51	50	47	45	48.8	50	20	30
D61-2013	49	54	53	49	51	51.2	51	30	21
D65-2013	TARPED CAGE								
D01-2014	TARPED CAGE								
D02-2014	51	54	54	47	52	51.6	50	25	25
D03-2014	52	56	50	46	54	51.6	52	30	22
D04-2014	55	49	47	50	52	50.6	53	31	22
D05-2014	TARPED CAGE								

	FLYOVER 2								
Donation #	1	2	3	4	5	Average	5x5	Perimeter	x-y=z
D06-2014	59	56	50	53	53	54.2	56	30	26
D07-2014	48	47	39	42	48	44.8	45	27	18
D08-2014	54	55	45	51	49	50.8	51	32	19
D09-2014	63	54	53	57	50	55.4	52	30	22
D10-2014	56	48	56	47	52	51.8	53	30	23
D11-2014	59	54	51	56	54	54.8	56	44	12
D12-2014	55	49	41	53	57	51	56	28	28
D13-2014	59	55	55	51	52	54.4	54	40	14
D14-2014	TARPED CAGE								
D15-2014	63	51	42	60	65	56.2	58	35	23
D16-2014	59	51	50	61	52	54.6	55	32	23
D17-2014	49	49	48	46	52	48.8	50	30	20
D19-2014	42	41	48	42	41	42.8	43	30	13
D20-2014	42	47	44	43	40	43.2	43	32	11
D21-2014	48	56	50	46	49	49.8	48	30	18
D23-2014						0			
D24-2014						0			
D25-2014						0			
D26-2014						0			
D27-2014						0			
D28-2014						0			
D29-2014	52	48	48	53	46	49.4	49	26	23
D30-2014						0			
D32-2014	56	68	57	61	55	59.4	59	33	26
D33-2014						0			

FLYOVER 2									
Donation #	1	2	3	4	5	Average	5x5	Perimeter	x-y=z
D35-2014						0			
D36-2014						0			
D37-2014						0			
N1	40	35	36	40	29	36	35	36	-1
N2						0	37	34	3
N3						0	38	36	2
N4						0	31	34	-3
N5						0	41	37	4
N6						0	41	36	5
T1						0			
T2						0			
T3						0			
T4						0			
T5						0			
T6						0			

APPENDIX E

BMI Data

TxState ID #	Compiled Stature (cm)	Compiled Weight (lbs)	Compiled Stature (m)	Compiled Weight (kg)	BMI
D10-2009	177.8	175	1.778	79.37866475	25.10962784
D20-2011	149.9	290	1.499	131.5417873	58.54104529
D21-2011	154.9	163	1.549	73.93555631	30.8141725
D22-2011	177.8	190	1.778	86.1825503	27.26188166
D03-2012	162.6	125	1.626	56.69904625	21.44542567
D04-2012	167.6	154	1.676	69.85322498	24.86786109
D06-2012	165.1	140	1.651	63.5029318	23.29698015
D10-2012	152.4	227	1.524	102.965468	44.33244294
D11-2012	180.34	220	1.8034	99.7903214	30.68345716
D13-2012	172.7	200	1.727	90.718474	30.41662763
D14-2012	167.6	135	1.676	61.23496995	21.79974836
D16-2012	177.8	260	1.778	117.9340162	37.3057328
D19-2012	170.2	165	1.702	74.84274105	25.83631514
D27-2012	162.56	150	1.6256	68.0388555	25.74717699
D29-2012	175.26	185	1.7526	83.91458845	27.31944386
D30-2012	182.9	230	1.829	104.3262451	31.18646612
D31-2012	167.6	125	1.676	56.69904625	20.18495219
D34-2012	177.8	158.4	1.778	71.84903141	22.72780029
D35-2012	162.6	240	1.626	108.8621688	41.17521729
D36-2012	167.64	300	1.6764	136.077711	48.42076995
D38-2012	182	200	1.82	90.718474	27.38753593
D39-2012	190	130	1.9	58.9670081	16.33435127
D41-2012	175.26	155	1.7526	70.30681735	22.88926378
D42-2012	182.88	282	1.8288	127.9130483	38.24568315
D43-2012	157	160	1.57	72.5747792	29.44329555
D44-2012	182.88	200	1.8288	90.718474	27.12459798
D46-2012	169.05	250	1.6905	113.3980925	39.68034131
D47-2012	173.95	220	1.7395	99.7903214	32.97915738
D48-2012	170.2	190	1.702	86.1825503	29.75090835
D49-2012	175.3	210	1.753	95.2543977	30.9971099
D50-2012	175.3	260	1.753	117.9340162	38.37737416
D02-2013	173.7	158	1.737	71.66759446	23.75325826
D03-2013	157.5	85	1.575	38.55535145	15.5425957
D05-2013	170.2	230	1.702	104.3262451	36.01425747
D06-2013	190.5	350	1.905	158.7573295	43.74655162
D07-2013	173.6	300	1.736	136.077711	45.15309806
D08-2013	165.1	125	1.651	56.69904625	20.80087514

TxState ID #	Compiled Stature (cm)	Compiled Weight (lbs)	Compiled Stature (m)	Compiled Weight (kg)	BMI
D11-2013	177.8	160	1.778	72.5747792	22.95737403
D13-2013	182.88	321	1.8288	145.6031508	43.53497976
D14-2013	172.2	124	1.722	56.24545388	18.96798212
D15-2013	162.6	140	1.626	63.5029318	24.01887676
D16-2013	172.2	300	1.722	136.077711	45.89027931
D17-2013	167.64	125	1.6764	56.69904625	20.17532081
D20-2013	182.88	185	1.8288	83.91458845	25.09025313
D22-2013	187.96	200	1.8796	90.718474	25.67821693
D23-2013	177.8	150	1.778	68.0388555	21.52253815
D24-2013	177.8	200	1.778	90.718474	28.69671754
D26-2013	190.5	180	1.905	81.6466266	22.49822655
D28-2013	182.88	200	1.8288	90.718474	27.12459798
D29-2013	157.48	140	1.5748	63.5029318	25.6060721
D30-2013	182.88	185	1.8288	83.91458845	25.09025313
D31-2013	180.34	228	1.8034	103.4190604	31.79921923
D33-2013	172.72	145	1.7272	65.77089365	22.04694832
D34-2013	170.18	230	1.7018	104.3262451	36.02272295
D35-2013	185.42	200	1.8542	90.718474	26.38654831
D36-2013	177.8	138	1.778	62.59574706	19.8007351
D39-2013	152.4	110	1.524	49.8951607	21.4826816
D46-2013	177.8	240	1.778	108.8621688	34.43606104
D47-2013	160.02	199	1.6002	90.26488163	35.25090611
D50-2013	182.88	160	1.8288	72.5747792	21.69967838
D51-2013	166.37	170	1.6637	77.1107029	27.85894261
D52-2013	182.88	180	1.8288	81.6466266	24.41213818
D54-2013	152.4	113	1.524	51.25593781	22.06857292
D56-2013	144.78	112	1.4478	50.80234544	24.23631669
D57-2013	172.72	120	1.7272	54.4310844	18.24575034
D59-2013	175.26	129	1.7526	58.51341573	19.04977437
D61-2013	185.42	160	1.8542	72.5747792	21.10923865
D65-2013	172.72	170	1.7272	77.1107029	25.84814631
D01-2014	152.4	124	1.524	56.24545388	24.21684108
D02-2014	162.56	240	1.6256	108.8621688	41.19548318
D05-2014	167.64	136	1.6764	61.68856232	21.95074904
D06-2014	175.3	200	1.753	90.718474	29.52105705
D07-2014	157.48	150	1.5748	68.0388555	27.43507725
D09-2014	170.18	98	1.7018	44.45205226	15.34881239
D11-2014	170.18	260	1.7018	117.9340162	40.72133899
D12-2014	167.64	220.88	1.6764	100.1894827	35.65059889
D13-2014	185.42	170	1.8542	77.1107029	22.42856606

TxState ID #	Compiled Stature (cm)	Compiled Weight (lbs)	Compiled Stature (m)	Compiled Weight (kg)	BMI
D14-2014	185.42	185	1.8542	83.91458845	24.40755718
D15-2014	172.72	160	1.7272	72.5747792	24.32766712
D16-2014	167.6	160	1.676	72.5747792	25.8367388
D17-2014	177.8	240	1.778	108.8621688	34.43606104
D19-2014	157.48	120	1.5748	54.4310844	21.9480618
D20-2014	183.00	178.50	1.83	80.96623805	24.17696499
D21-2014	165.1	300	1.651	136.077711	49.92210033
D23-2014	175.30	174.00	1.753	78.92507238	25.68331963
D24-2014	175.26	173.50	1.7526	78.6982762	25.62120816
D25-2014	175.26	240	1.7526	108.8621688	35.44144069
D26-2014	188.00	186.00	1.88	84.36818082	23.87058081
D27-2014	180.34	180.00	1.8034	81.6466266	25.10464676
D28-2014	152.40	154.00	1.524	69.85322498	30.07575424
D29-2014	182.90	181.00	1.829	82.10021897	24.5423929
D30-2014	154.90	153.50	1.549	69.6264288	29.01825447
D33-2014	187.96	187.50	1.8796	85.04856938	24.07332838
D35-2014	165.10	188.00	1.651	85.27536556	31.28451621

WORKS CITED

- Aitkenhead-Peterson JA, Owings CG, Alexander MB, Larison N, and Bytheway JA. 2012. Mapping the lateral extent of human cadaver decomposition with soil chemistry. *Forensic science international* 216(1-3):127-134.
- Ajay Bedi AKS, Aman Gupta, Amit Kumar, Avinaash Gupta, Durga Ganesh Grandhi, Gagan Singhal, Kamal Arora, Krishna Singh Karki, Manoj Awasthi, Mohit Gupta, Nishant Gupta, Dishant Kumar, Phaneendra Angara, Sylvain Paris. 2013. Adobe Photoshop Elements 12. 12.0 (20130903.r.43239) x64 ed: Adobe Systems Incorporated.
- Ben-Dor E, Inbar Y, and Chen Y. 1997. The Reflectance Spectra of Organic Matter in the Visible Near-Infrared and Short Wave Infrared Region (400-2500 nm) during a Controlled Decomposition Process. *Remote Sensing of Environment* 61:1-15.
- Benninger LA, Carter DO, and Forbes SL. 2008. The biochemical alteration of soil beneath a decomposing carcass. *Forensic science international* 180(2-3):70-75.
- Bohun CS, Barons MJ, Gideon A, Khan ZH, Ranner T, and Smith N. 2010. Modelling a Cadaver Decomposition Island to Estimate Time of Death. p 1-12.
- Bot A, Benites J, Food, and Nations AOotU. 2005. The Importance of Soil Organic Matter: Key to Drought-resistant Soil and Sustained Food Production: Food and Agriculture Organization of the United Nations.
- Carter DO, Yellowlees D, and Tibbett M. 2007. Cadaver decomposition in terrestrial ecosystems. *Die Naturwissenschaften* 94(1):12-24.
- FAA. 2014. Busting Myths about the FAA and Unmanned Aircraft. Federal Aviation Administration: Federal Aviation Administration.

- Francescani C. 2013. Domestic drones are already reshaping U.S. crime-fighting.
Reuters. Reuters: Thomson Reuters.
- Kalacska M, and Bell LS. 2006. Remote Sensing as a Tool for the Detection of
Clandestine Mass Graves. *Canadian Society of Forensic Science* 39(1):1-13.
- Kalacska ME, Bell LS, Arturo Sanchez-Azofeifa G, and Caelli T. 2009. The Application
of Remote Sensing for Detecting Mass Graves: An Experimental Animal Case
Study from Costa Rica*. *Journal of forensic sciences* 54(1):159-166.
- McLellan TM, Aber JD, and Martin ME. 1991. Determination of nitrogen, lignin, and
cellulose content of decomposing leaf material by near infrared reflectance
spectroscopy. *Canadian Journal of Forest Research* 21:1684-1688.
- Nagy NM, and Konya J. 2009. *Interfacial chemistry of rocks and soils*. Boca Raton, Fla.;
London: CRC ; Taylor & Francis [distributor].
- Parks CL. 2011. A Study of the Human Decomposition Sequence in Central Texas*.
Journal of forensic sciences 56(1):19-22.
- Price J. 1994. How unique are spectral signatures? *Remote Sensing of Environment*
49(3):181-186.
- Reed HB, Jr. 1958. A Study of Dog Carcass Communities in Tennessee, with Special
Reference to the Insects. *American Midland Naturalist* 59(1):213-245.
- Rodriguez WC, and Bass WM. 1983. Insect Activity and its Relationship to Decay Rates
of Human Cadavers in East Tennessee. *Journal of forensic sciences* 28(2):423.

- Ruffell A, McCabe A, Donnelly C, and Sloan B. 2009. Location and Assessment of an Historic (150–160 Years Old) Mass Grave Using Geographic and Ground Penetrating Radar Investigation, NW Ireland*. *Journal of forensic sciences* 54(2):382-394.
- Snirer E. 2013. *Hyperspectral Remote Sensing of Individual Gravesites - Exploring the effects of Cadaver Decomposition on Vegetation and Soil Spectra*: McGill University. 122 p.
- Statheropoulos M, Spiliopoulou C, and Agapiou A. 2005. A study of volatile organic compounds evolved from the decaying human body. *Forensic science international* 153(2-3):147-155.
- Tibbett M, and Carter DO. 2008. *Soil analysis in forensic taphonomy: chemical and biological effects of buried human remains*: CRC Press.
- Towne EG. 2000. Prairie vegetation and soil nutrient responses to ungulate carcasses. *Oecologia* 122:232-239.
- Vass AA, Bass WM, Wolt JD, Foss JE, and Ammons JT. 1992. Time since death determinations of human cadavers using soil solution. *Journal of forensic sciences* 37(5):1236-1253.
- Xie Y, Sha Z, and Yu M. 2008. Remote sensing imagery in vegetation mapping: a review. *Journal of plant ecology* 1(1):9-23.